Reflection and transmission through a microstructured slab sandwiched by two half-spaces

Article *in* European Journal of Mechanics - A/Solids · December 2015

DOI: 10.1016/j.euromechsol.2015.11.005

2 authors, including:

Peijun Wei
University of Science and Technology Beijing
72 PUBLICATIONS **280** CITATIONS

SEE PROFILE

European Journal of Mechanics A/Solids 57 (2016) 1–17

Contents lists available at ScienceDirect

European Journal of Mechanics A/Solids

journal homepage: www.elsevier.com/locate/ejmsol

Reflection and transmission through a microstructured slab sandwiched by two half-spaces

Yueqiu Li [a], Peijun Wei [a, b, *]

[a] Department of Applied Mechanics, University of Sciences and Technology Beijing, Beijing 100083, China
[b] State Key Laboratory of Nonlinear Mechanics (LNM), Chinese Academy of Science, Beijing, China

ARTICLE INFO

Article history:
Received 12 May 2015
Accepted 16 November 2015
Available online 2 December 2015

Keywords:
Reflection and transmission
Gradient elasticity
Sandwiched slab

ABSTRACT

The reflection and transmission of a plane wave through a microstructured slab sandwiched by two half-spaces are studied in this paper. First, the wave propagation in a micro-structured solid of the dipolar gradient elasticity is formulated. Then, the reflection and transmission properties of a plane wave through a micro-structured slab sandwiched by two half-spaces are considered. The nontraditional interfacial conditions by requiring the auxiliary monopolar tractions, the auxiliary dipolar tractions, the displacements and the normal derivative of displacements continuous across the two interfaces are used to determine the amplitude ratio. The energy fluxes carried by various waves and the reflection and transmission coefficients in terms of energy flux ratio with respect to incident wave are calculated numerically. Based on these numerical results, the microstructure effects on the reflection and transmission waves for the incident P wave and incident SH wave with different wavelength are discussed. In particular, the influences of three characteristic lengths, namely, the incident wavelength, the thickness of slab and the characteristic length of microstructure, on the reflection and transmission waves are analyzed. It is found that the microstructure effect results in the appearance of evanescent wave mode. The reflection and transmission coefficients are evidently dependent upon the microstructure parameters and become more pronounced when the incident wavelength is close to the characteristic length of microstructure.

1. Introduction

It is known that the classical elastic theory do not suffice for an accurate and detailed description of corresponding mechanical behavior in the range of micro and nano-scales. The main cause is the absence of an internal length, characteristic of the underlying microstructure, from the constitutive equation in the classical elastic theory, and therefore the notable size effects observed experimentally with newly developed probes such as nano-indenters and atomic force microscopes could not be captured (see Fleck et al., 1994; Stölken and Evans, 1998; Chong and Lam, 1999; McFarland and Colton, 2005). In the problem of wave propagation, the classical elastic theory is also believed to be inadequate for a material possessing microstructure, in particular, when the wavelength of an incident wave is comparable to the length of the material microstructure. In order to take the microstructure effects into consideration, the generalized continuum theories, for example, the couple stress theory (Mindlin and Tiersten, 1962, Toupin, 1962), the micromorphic theory (Eringen, 1964), the micropolar theory (Eringen, 1966), micro-stretch theory (Eringen, 1990) and the nonlocal theory (Eringen, 2001), were proposed successively. Because the freedom degree of the material particle increases in these generalized continuum theories, the modes of vibration of material particle become more complicated and therefore create many new wave modes which cannot be observed in the classical elastic solids. Parfitt and Eringen (1969) and Tomar and Gogna (1995) have shown that there are four basic waves travelling at four distinct phase velocities in an infinite micropolar solid. They are the longitudinal displacement wave (LD), the longitudinal microrotation wave (LR), the transverse displacement wave (TD) and the transverse microrotation wave (TR). Mindlin (1964) proposed a linear elastic theory of solid with microstructure where macromotion and micromotion coexist and showed that there are four micro-vibration modes. The coupling between the macro-vibration and

* Corresponding author. Department of Applied Mechanics, University of Sciences and Technology Beijing, Beijing 100083, China.
E-mail address: weipj@ustb.edu.cn (P. Wei).

http://dx.doi.org/10.1016/j.euromechsol.2015.11.005
0997-7538/

the micro-vibration leads to twelve kinds of wave modes. Eight of them are the dispersive. Too many motion freedoms and material parameters make the application of these microstructure elastic theories restricted. In contrast, the gradient elastic theory has less material parameters and therefore attracted wide attentions in the last two decades. Askes and Aifantis (2011) gave a comprehensive and detailed review of various gradient elasticity formats including the multi-scale format and the mono-scale format, the stress gradient format and the strain gradient format, the stable strain gradient format and the unstable strain gradient format and so on. However, many of these gradient elasticity theories are out of the context of the rigorous theories of Toupin (1962) and Mindlin (1964). Georgiadis et al. (2004) initially derived the dipolar gradient elasticity with consideration of surface energy. Only two microstructure parameters are included in this gradient theory and three extra surface parameters are added when the surface energy effect is considered. This gradient theory predicts the dispersive properties of Rayleigh surface wave propagating along the surface of half-space. Gourgiotis et al. (2013) further studied the reflection problem of plane waves on a plane boundary of half-space governed by the gradient elasticity. Their investigations showed that there are only four wave modes in the gradient elastic solid considered. Two of them are P wave (the dilatational or longitudinal wave) and SV wave (the distortional or transverse wave); other two of them are the evanescent waves which reduce to the P type and S type surface waves at a boundary. These waves are all dispersive. Arkadi and Mihhail (2013) also studied the influences of material microstructure on the reflection of thermoelastic wave based on the gradient elasticity. Compared with the reflection and transmission through an interface, the reflection and transmission problem through a slab will concern two interfaces and a geometrical characteristic length, namely, the thickness of slab. Giacomo and Angelo (2008, 2012) studied the wave propagation through an elastic slab and a viscoelastic slab, respectively. Tolokonnikov (1998) studied the wave propagation through an inhomogeneous anisotropic slab. Larin and Tolokonnikov (2006) further studied the wave propagation through a non-uniform thermoelastic slab. In particular, if the slab is a solid with microstructure, then, there are two external characteristic lengths and one internal characteristic length to be considered. Although the reflection and transmission through a slab characteristic of the classical elasticity had been studied, the study on the wave propagation through a slab with microstructure is less reported. Recently, Hsia and Su (2008) studied the wave propagation through a microporous slab characteristic of micropolar elasticity. Khurana and Tomar (2009) studied the wave propagation through a chiral slab characteristic of non-centrosymmetry. The effects of chirality parameters on the reflection and transmission were discussed. However, only the displacement amplitude ratios were calculated while the energy flux densities carried by various waves were not calculated. And therefore the numerical results are obtained without validation by the energy flux conservation.

In this paper, the reflection and transmission of in-plane and out-of-plane elastic waves through a slab sandwiched between two elastic or gradient elastic half-spaces are studied. The slab is characteristic of the dipolar gradient elasticity. The dipolar gradient elastic theory is derived from the linear elastic theory of microstructured solids proposed by Mindlin based on some hypothesis. The non-traditional interfacial conditions at two interfaces are used to determine the displacement amplitude ratios of various reflection and transmission waves with respect to the incident wave. The energy fluxes carried by various waves are calculated and used to validate the numerical results. The influences of the microstructure parameters on the reflection and transmission waves with consideration of three characteristic lengths, namely, the incident wavelength, the thickness of slab and the characteristic length of microstructure, are discussed based on the numerical results.

2. Simplified formulation of dipolar gradient elasticity

According to the Mindlin's elastic theory of solids with microstructure, the strain energy density can be expressed as

$$W = \frac{1}{2}c_{ijkl}\varepsilon_{ij}\varepsilon_{kl} + \frac{1}{2}b_{ijkl}\gamma_{ij}\gamma_{kl} + \frac{1}{2}a_{ijklmn}\chi_{ijk}\chi_{lmn} + d_{ijklm}\gamma_{ij}\chi_{klm} + f_{ijklm}\chi_{ijk}\varepsilon_{lm} + g_{ijkl}\gamma_{ij}\varepsilon_{kl}, \tag{1}$$

where c_{ijkl}, b_{ijkl}, a_{ijklmn}, d_{ijklm}, f_{ijklm} and g_{ijkl} are the components of elastic tensor. ε_{ij}, $\gamma_{ij}(=u_{j,i} - \psi_{ij})$ and $\chi_{ijk}(=\psi_{jk,i})$ are the macro-strain of macro-medium, relative deformation (the difference between the macro-displacement gradient and the micro-deformation) and the micro-deformation gradient (the macro-gradient of the micro-deformation), respectively. If the relative deformation is ignored, namely, $\gamma_{ij} = 0$, then, the strain energy density function is simplified as

$$W = \frac{1}{2}c_{ijkl}\varepsilon_{ij}\varepsilon_{kl} + \frac{1}{2}a_{ijklmn}\chi_{ijk}\chi_{lmn} + f_{ijklm}\chi_{ijk}\varepsilon_{lm}. \tag{2}$$

It means that the strain energy density is dependent of the strain not only but also the strain gradient. Even for isotropic and centrosymmetric medium, there are too many material constants involved. A phenomenological simplified version is given as following.

$$W = \left(\frac{1}{2}\lambda\varepsilon_{ii}\varepsilon_{jj} + \mu\varepsilon_{ij}\varepsilon_{ij}\right) + \left(\frac{1}{2}\lambda c\varepsilon_{ii,k}\varepsilon_{jj,k} + \mu c\varepsilon_{ij,k}\varepsilon_{ji,k,}\right) \tag{3}$$

where the first term is the contribution from the strains; the second term is the contribution from the strain gradient. This form of strain energy density without consideration of surface effects is first given by Georgiadis et al. (2004). Define

$$\tau_{ij} = \frac{\partial W}{\partial \varepsilon_{ij}} = \left(\lambda\delta_{ij}\varepsilon_{pp} + 2\mu\varepsilon_{ij}\right), \tag{4a}$$

$$\mu_{kij} = \frac{\partial W}{\partial \chi_{kij}} = c\left(\lambda\delta_{ij}\varepsilon_{pp,k} + 2\mu\varepsilon_{ij,k}\right), \tag{4b}$$

where λ and μ are the classic lame constants; c is a microstructure parameter with dimension of m^2; τ_{ij} is the Cauchy stress or monopolar stress while μ_{ijk} is the dipolar stress with the dimensions of Nm^{-1}. The monopolar stress and the dipolar stress are corresponding with the notion of monopolar force and the dipolar force, respectively. The monopolar forces are the classical forces and the dipolar forces are the anti-parallel forces acting between the micro-media contained in the continuum with microstructure. It is noted that there are a microstructure parameter c involved in the constitutive equations. Therefore, the microstructure effects can be captured to a certain extent.

The kinetic energy density includes two terms. One involves the velocity, and the other term involves the velocity gradient

$$T = \frac{1}{2}\rho\dot{u}_j\dot{u}_j + \frac{1}{6}\rho d^2\dot{u}_{k,j}\dot{u}_{k,j}. \tag{5}$$

where ρ is the mass density and d is the characteristic length of microstructure.

The work done by the external forces is

$$W_1 = \int_V F_k u_k dV + \int_S P_k u_k dS + \int_S R_k D u_k dS, \tag{6}$$

where F_k is the body force. P_k is the monopolar traction. R_k is the dipolar tractions.

Hamilton variational principle requires

$$\delta \int_{t_0}^{t_1} \int_V (T - W) dV dt + \int_{t_0}^{t_1} \int_S \delta W_1 dS dt = 0, \tag{7}$$

which leads to the motion equation and the boundary condition

$$\left(\tau_{jk} - \mu_{ijk,i}\right)_{,j} + F_k = \rho \ddot{u}_k - \frac{\rho d^2}{3} \ddot{u}_{k,jj}, \quad \text{in V} \tag{8}$$

$$P_k = n_j\left(\tau_{jk} - \mu_{ijk,i}\right) - D_j\left(n_i \mu_{ijk}\right) + (D_l n_l) n_i n_j \mu_{ijk} + \frac{\rho d^2}{3} n_j \ddot{u}_{k,j}, \quad \text{on surface} \tag{9}$$

$$R_k = n_i n_j \mu_{ijk}, \quad \text{on surface} \tag{10}$$

where n_j is the normal of the boundary of solid. $D_j = (\delta_{jl} - n_j n_l)\partial_l$, $D = n_l \partial_l$.

3. Reflection and transmission through a microstructured slab

Inserting Eqs. (3) and (4) into Eq. (8) and ignoring the volume force leads to the equation of motion in terms of displacement.

$$\left(1 - c\nabla^2\right)\left[(\lambda + \mu)\nabla\nabla\cdot\mathbf{u} + \mu\nabla^2\mathbf{u}\right] = \rho\ddot{\mathbf{u}} - \frac{\rho d^2}{3}\nabla^2\ddot{\mathbf{u}}, \tag{11}$$

where ∇^2 is the Laplace operator. Eq. (11) reduces to Navier equation in the classical elastic theory when the microstructure parameter c and d are taken to be zero. It is noted that the microstructure parameter c and d appear in the equation. It means that the microstructure effects will influence the wave propagation modes in the solid.

In the case of in-plane incident wave (P or SV wave), the application of Helmholtz vector decomposition

$$\mathbf{u}(x,y) = u_x(x,y)\mathbf{e}_x + u_y(x,y)\mathbf{e}_y = \nabla\varphi(x,y) + \nabla \times \psi(x,y)\mathbf{e}_z, \tag{12}$$

leads to

$$\left(\nabla^2 + \sigma_p^2\right)\left(\nabla^2 - \tau_p^2\right)\varphi = 0, \tag{13a}$$

$$\left(\nabla^2 + \sigma_s^2\right)\left(\nabla^2 - \tau_s^2\right)\psi = 0, \tag{13b}$$

Eq. (13) means that there are two travelling waves of wave number σ_p and σ_s and two evanescent waves with imaginary wavenumber or attenuation factor τ_p and τ_s. In the reflection and transmission problem, the apparent wave number of all waves (incident waves, reflection waves and transmission waves) should be equal. Let us consider the solutions of form

$$\varphi(x,y,t) = \widetilde{\varphi}(y)\exp[i(\xi x - \omega t)], \tag{14a}$$

$$\psi(x,y,t) = \widetilde{\psi}(y)\exp[i(\xi x - \omega t)], \tag{14b}$$

Inserting Eq. (14) into Eq. (13) leads to

$$\left(\frac{d^2}{dy^2} + \beta_p^2\right)\left(\frac{d^2}{dy^2} - \gamma_p^2\right)\widetilde{\varphi}(y) = 0, \tag{15a}$$

$$\left(\frac{d^2}{dy^2} + \beta_s^2\right)\left(\frac{d^2}{dy^2} - \gamma_s^2\right)\widetilde{\psi}(y) = 0, \tag{15b}$$

where

$$\beta_p^2 = \sigma_p^2 - \xi^2,\ \gamma_p^2 = \tau_p^2 + \xi^2,\ \beta_s^2 = \sigma_s^2 - \xi^2,\ \gamma_s^2 = \tau_s^2 + \xi^2,\ \sigma_p = \left\{\frac{1}{2c}\left[\Delta_p - (1-a)\right]\right\}^{\frac{1}{2}},$$

$$\tau_p = \left\{\frac{1}{2c}\left[\Delta_p + (1-a)\right]\right\}^{\frac{1}{2}},\ \sigma_s = \left\{\frac{1}{2c}\left[\Delta_s - (1-m)\right]\right\}^{\frac{1}{2}},\ \tau_s = \left\{\frac{1}{2c}\left[\Delta_s + (1-m)\right]\right\}^{\frac{1}{2}},$$

$$a = \frac{\omega^2 d^2}{3V_p^2},\ m = \frac{\omega^2 d^2}{3V_s^2},\ \Delta_p = \left[(1-a)^2 + \frac{4c\omega^2}{V_p^2}\right]^{\frac{1}{2}},\ \Delta_s = \left[(1-m)^2 + \frac{4c\omega^2}{V_s^2}\right]^{\frac{1}{2}},$$

$$V_p^2 = \frac{\lambda + 2\mu}{\rho},\ V_s^2 = \frac{\mu}{\rho}.$$

It is noted that both γ_p^2 and γ_s^2 always are real values greater than zero. Whereas β_p^2 and β_s^2 may have real values greater than, equal to, or less than zero. In the case of $\beta_p^2 > 0$ and $\beta_s^2 > 0$,

$$\varphi = A_1 \exp\left[i(\xi x - \beta_p y - \omega t)\right] + A_2 \exp\left[i(\xi x + \beta_p y - \omega t)\right] + C_1 \exp\left[+\gamma_p y + i(\xi x - \omega t)\right] + C_2 \exp\left[-\gamma_p y + i(\xi x - \omega t)\right], \tag{16a}$$

$$\psi = B_1 \exp[i(\xi x - \beta_s y - \omega t)] + B_2 \exp[i(\xi x + \beta_s y - \omega t)] + D_1 \exp[+\gamma_s y + i(\xi x - \omega t)] + D_2 \exp[-\gamma_s y + i(\xi x - \omega t)]. \tag{16b}$$

Consider an incident plane P or SV wave from medium1 propagates obliquely toward a slab (of a thickness h) sandwiched by two half-planes, see Fig. 1. The two half-planes are indicated by medium 1 and medium 3, respectively. The slab is indicated by medium 2 which is a homogenous medium of different microstructured from medium 1 and medium3. Their material constants are $(\nu_i,\mu_i,\rho_i,c_i,d_i)$ $(i = 1,2,3)$, respectively. According to Eq. (16), the incident waves, the reflection waves and the transmission waves can be expressed as (the time factor $\exp(-i\omega t)$ is suppressed for brevity)

$$\varphi_1 = A_0 \exp\left[i\sigma_{p1}(\sin\theta_1 x + \cos\theta_1 y)\right], \tag{17a}$$

$$\psi_1 = B_0 \exp[i\sigma_{s1}(\sin\theta_2 x + \cos\theta_2 y)], \tag{17b}$$

for incident P wave and SV wave.

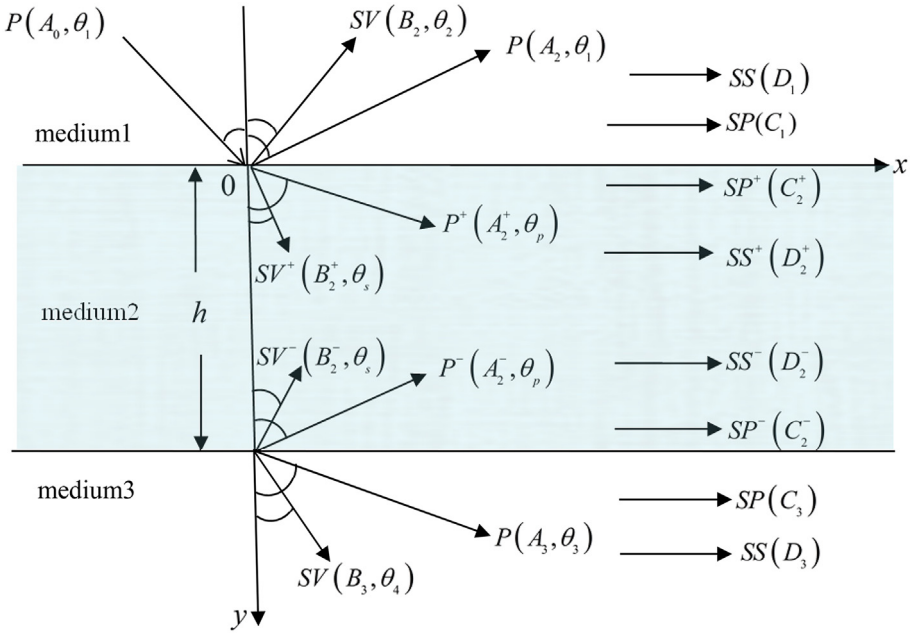

Fig. 1. Reflection and transmission through a microstructured slab sandwiched by two elastic or gradient elastic half-spaces.

$$\varphi_1 = A_1 \exp\left[i\sigma_{p1}(\sin\theta_1 x - \cos\theta_1 y)\right] + C_1 \exp(i\sigma_{p1}\sin\theta_1 x + \gamma_{p1} y), \tag{18a}$$

$$\psi_1 = B_1 \exp[i\sigma_{s1}(\sin\theta_2 x - \cos\theta_2 y)] + D_1 \exp(i\sigma_{s1}\sin\theta_2 x + \gamma_{s1} y), \tag{18b}$$

for the reflection P wave, SV wave and two surface waves.

$$\varphi_3 = A_3 \exp\left[i\sigma_{p3}(\sin\theta_3 x + \cos\theta_3 y)\right] + C_3 \exp(i\sigma_{p3}\sin\theta_3 x - \gamma_{p3} y), \tag{19a}$$

$$\psi_3 = B_3 \exp[i\sigma_{s3}(\sin\theta_4 x + \cos\theta_4 y)] + D_3 \exp(i\sigma_{s3}\sin\theta_4 x - \gamma_{s3} y), \tag{19b}$$

for the transmission P wave, SV wave and two surface waves.

In the medium 2, there are two sets of waves. One of them is the transmission waves at the interface between medium 1 and medium2 and the other is the reflection waves at the interface between medium 2 and medium 3. These waves can be expressed as

$$\begin{aligned}\varphi_2 = {} & A_2^+ \exp\left[i\sigma_{p2}(\sin\theta_p x + \cos\theta_p y)\right] + C_2^+ \exp(i\sigma_{p2}\sin\theta_p x \\ & - \gamma_{p2} y) + A_2^- \exp\left[i\sigma_{p2}(\sin\theta_p x - \cos\theta_p y)\right] \\ & + C_2^- \exp(i\sigma_{p2}\sin\theta_p x + \gamma_{p2} y),\end{aligned} \tag{20a}$$

$$\begin{aligned}\psi_2 = {} & B_2^+ \exp[i\sigma_{s2}(\sin\theta_s x + \cos\theta_s y)] + D_2^+ \exp(i\sigma_{s2}\sin\theta_s x \\ & - \gamma_{s2} y) + B_2^- \exp[i\sigma_{s2}(\sin\theta_s x - \cos\theta_s y)] \\ & + D_2^- \exp(i\sigma_{s2}\sin\theta_s x + \gamma_{s2} y),\end{aligned} \tag{20b}$$

where A_i^j and B_i^j represent the amplitudes of bulk waves and C_i^j and D_i^j represent the amplitudes of the evanescent waves. The subscript $i = 0$ indicates the incident wave and $i = 1,2,3$ indicates the waves in the medium 1, medium 2 and medium3, respectively. The superscript $j = +$ on the propagating waves indicates the forward propagating waves which propagate toward to the interface between medium 2 and medium 3; and $j = -$ represent the backward propagating waves which propagate toward to the interface between medium 2 and medium1. There are also two sets of evanescent waves in the medium 2. Both of them propagate along positive x direction. One set of them propagates near top boundary and the other propagates near the low boundary. In order to distinguish these two sets of evanescent waves, we still use $(+)$ sign and $(-)$ sign. Therefore, $(+)$ sign and $(-)$ sign on the evanescent waves only represent that they are associated with the forward and backward propagating wave, respectively. These amplitudes should be determined by the continuous conditions at two interfaces. Different from the classical elastic solid, the continuous conditions of displacement components and traction components are replaced by

$$\left(u_i^{(1)} - u_i^{(2)}\right)\Big|_{y=0} = 0, \quad \left(n_y u_{i,y}^{(1)} - n_y u_{i,y}^{(2)}\right)_{y=0} = 0, \ (i = x, y) \tag{21a,b}$$

$$\left(P_i^{(1)} - P_i^{(2)}\right)\Big|_{y=0} = 0, \quad \left(R_i^{(1)} - R_i^{(2)}\right)\Big|_{y=0} = 0. \tag{21c,d}$$

$$\left(u_i^{(2)} - u_i^{(3)}\right)\Big|_{y=h} = 0, \quad \left(n_y u_{i,y}^{(2)} - n_y u_{i,y}^{(3)}\right)\Big|_{y=h} = 0, \tag{22a,b}$$

$$\left(P_i^{(2)} - P_i^{(3)}\right)\Big|_{y=h} = 0, \quad \left(R_i^{(2)} - R_i^{(3)}\right)\Big|_{y=h} = 0. \tag{22c,d}$$

where

$$P_x = 2\mu\left(1 - c\nabla^2\right)\varepsilon_{yx} - c\left[(\lambda + 2\mu)\varepsilon_{xx,x} + \lambda\varepsilon_{yy,x}\right]_y + \frac{\rho d^2}{3}\ddot{u}_{x,y}$$

$$P_y = \left(1 - c\nabla^2\right)\left[(\lambda + 2\mu)\varepsilon_{yy} + \lambda\varepsilon_{xx}\right] - 2\mu c\varepsilon_{xy,xy} + \frac{\rho d^2}{3}\ddot{u}_{y,y}$$

$R_x = 2\mu c\varepsilon_{yx,y}$, $R_y = c\left[(\lambda+2\mu)\varepsilon_{yy}+\lambda\varepsilon_{xx}\right]_{,y}$,

The interfacial conditions Eqs. (21) and (22) mean that the displacement, the normal derivative of displacement, the monopolar traction and the dipolar tractions are continuous across each interface. The interface conditions require that the apparent wavenumbers are same for incident wave, reflection and transmission waves. This gives the relation between incident angle, reflection angles and transmission angles.

$$\sigma_{p1}\sin\theta_1 = \sigma_{s1}\sin\theta_2 = \sigma_{p3}\sin\theta_3 = \sigma_{s3}\sin\theta_4 = \sigma_{p2}\sin\theta_p = \sigma_{s2}\sin\theta_s.$$

When medium 1 and medium 3 are the classical elastic solids, the interface conditions reduces to

$$\left(u_i^{(1)}-u_i^{(2)}\right)\Big|_{y=0}=0 \quad \left(P_i^{(2)}-\tau_{ij}^{(1)}n_j\right)\Big|_{y=0}=0 \quad \left(R_i^{(2)}\right)\Big|_{y=0}=0 \quad (i=x,y) \tag{23a,b,c}$$

$$\left(u_i^{(2)}-u_i^{(3)}\right)\Big|_{y=h}=0, \quad \left(P_i^{(2)}-\tau_{ij}^{(3)}n_j\right)\Big|_{y=h}=0, \quad \left(R_i^{(2)}\right)\Big|_{y=h}=0. \tag{24a,b,c}$$

It should be pointed out that letting the normal derivatives of the displacements to be zero ($n_y u_{i,y}^{(2)}=0$) instead of the dipolar tractions $R_i^{(2)}=0$ in Eqs. (23) and (24) is also possible option. Because the normal derivatives of the displacements and the dipolar tractions are both related to the microstructure effects, the two sets of interface conditions reflect two kinds of different microstructure of interfaces, in fact.

Eqs. (21) and (22) can be rewritten in the matrix form

$$\mathbf{Ax}=\mathbf{B}, \tag{25}$$

where

$$\mathbf{x}=\left(A_1,C_1,B_1,D_1,A_2^+,C_2^+,A_2^-,C_2^-,B_2^+,D_2^+,B_2^-,D_2^-,A_3,C_3,B_3,D_3\right)\times\Big/A_0.$$

In the case of out-of plane incident wave (SH wave), inserting $\mathbf{u}=u_z(x,y)\mathbf{e}_z$ directly into Eq. (11) leads to

$$\left(\nabla^2+\sigma_{sh}^2\right)\left(\nabla^2-\tau_{sh}^2\right)\mathbf{u}=0 \tag{26}$$

where

$$\sigma_{sh}=\left\{\frac{1}{2c}[\Delta_s-(1-m)]\right\}^{\frac{1}{2}},\ \tau_{sh}=\left\{\frac{1}{2c}[\Delta_s+(1-m)]\right\}^{\frac{1}{2}},\ m=\frac{\omega^2d^2}{3V_s^2},\ \Delta_s=\left[(1-m)^2+\frac{4c\omega^2}{V_s^2}\right]^{\frac{1}{2}}.$$

Eq. (26) implies that there are a SH bulk wave and a SH type surface wave (called SSH wave for brevity) in a gradient elastic medium. Accordingly, the displacement field in the medium 1, medium 2 and medium 3 can be expressed as

$$u^{(1)}=H_0\exp[i\sigma_{sh1}(\sin\theta_1x+\cos\theta_1y)]+H_1\exp[i\sigma_{sh1}(\sin\theta_1x-\cos\theta_1y)]+F_1\exp(\gamma_{sh1}y+i\sigma_{sh1}\sin\theta_1x), \tag{27a}$$

$$u^{(2)}=H_2^+\exp[i\sigma_{sh2}(\sin\theta_sx+\cos\theta_sy)]+F_2^+\exp(-\gamma_{sh2}y+i\sigma_{sh2}\sin\theta_sx)+H_2^-\exp[i\sigma_{sh2}(\sin\theta_sx-\cos\theta_sy)]+F_2^-\exp(\gamma_{sh2}y+i\sigma_{sh2}\sin\theta_sx), \tag{27b}$$

$$u^{(3)}=H_3\exp[i\sigma_{sh3}(\sin\theta_2x+\cos\theta_2y)]+F_3\exp(-\gamma_{sh3}y+i\sigma_{sh3}\sin\theta_2x). \tag{27c}$$

where H_0, H_1, H_2 and H_3 are the amplitudes of bulk waves; F_1, F_2 and F_3 are the amplitudes of surface waves (called SSH wave for brevity). The interface conditions can be expressed as

$$\left(u_z^{(1)}-u_z^{(2)}\right)\Big|_{y=0}=0, \quad \left(n_yu_{z,y}^{(1)}-n_yu_{z,y}^{(2)}\right)\Big|_{y=0}=0, \tag{28a,b}$$

$$\left(P_z^{(1)}-P_z^{(2)}\right)\Big|_{y=0}=0, \quad \left(R_z^{(1)}-R_z^{(2)}\right)\Big|_{y=0}=0. \tag{28c,d}$$

$$\left(u_z^{(2)}-u_z^{(3)}\right)\Big|_{y=h}=0, \quad \left(n_yu_{z,y}^{(2)}-n_yu_{z,y}^{(3)}\right)\Big|_{y=h}=0, \tag{29a,b}$$

$$\left(P_z^{(2)}-P_z^{(3)}\right)\Big|_{y=h}=0, \quad \left(R_z^{(2)}-R_z^{(3)}\right)\Big|_{y=h}=0. \tag{29c,d}$$

where

$$P_z=2\mu\left[\varepsilon_{yz}-c\left(\nabla^2\varepsilon_{yz}+\varepsilon_{xz,xy}\right)\right]+\frac{\rho d^2}{3}\ddot{u}_{z,y} \quad R_z=2\mu c\varepsilon_{yz,y}.$$

These interface conditions can also be rewritten into matrix form, as Eq. (25).

The explicit expression of the elements of matrix **A** and **B** in the case of incident P wave are listed in the appendix a and that in the case of incident SH wave are not given here for brevity but can be obtained similarly. It is noted that the matrix **A** is of dimension 16 × 16 in the case of incident P wave and 8 × 8 in the case of incident SH wave. When the two half-spaces are both classic elastic media, the matrix **A** is of dimension 12 × 12 in the case of incident P wave and 6 × 6 in the case of incident SH wave. The amplitude ratio **x** for various incident waves can be obtained by solving Eq. (25).

It is known that the amplitude ratio **x** is dependent upon the material constants of three media ($\nu_i,\mu_i,\rho_i,c_i,d_i$) and the incident wave parameters ($A_0,\lambda,\omega,\theta$). In order to simplify the analysis, it is assumed that medium 1 and medium 3 are identical in this paper. Thus, the dependence of reflection and transmission upon the material constants and incident wave parameters may be expressed as

$$(A_i,B_i,C_i,D_i)=f(\nu_1,\mu_1,\rho_1,c_1,d_1,\nu_2,\mu_2,\rho_2,c_2,d_2,A_0,\lambda,\omega,\theta,h). \tag{30}$$

Choose (ρ_2,d_2,ω) as the basic physical quantities, then, the nondimensional form of Eq. (30) is

$$(A_i,\ B_i,C_i,D_i)/A_0=f\left(\nu_1,\alpha_1,\overline{d},\nu_2,\overline{\mu},\overline{\rho},\alpha_2,\overline{\lambda},\theta,\overline{h}\right), \tag{31}$$

where ν_i is the Poisson ratio of material, λ is the incident wavelength (not confused with the Lame constants). Besides,

$$\alpha_1 = \frac{\sqrt{c_1}}{d_1},\ \overline{d} = \frac{d_1}{d_2},\ \overline{\mu} = \frac{\mu_1}{\mu_2},\ \overline{\rho} = \frac{\rho_1}{\rho_2},\ \alpha_2 = \frac{\sqrt{c_2}}{d_2},\ \overline{\lambda} = \frac{\lambda}{d_2},\ \overline{h} = \frac{h}{\lambda}.$$

Although the amplitude ratios of reflection and transmission waves can be obtained from Eq. (25), the propagation process through a slab and the formation of resulting reflection and transmission waves are concealed by Eq. (25). In order to present a clearer physical picture of wave propagation through a slab and of the formation of resulting reflection and transmission waves, we appeal to the multiply reflection and transmission approach.

In the case of incident SH wave, there is no mode conversion. Therefore, the reflection and transmission SH waves can be obtained by

$$H^{\mathrm{R}} = R_{12}H^{\mathrm{I}} + T_{21}R_{23}T_{12}H^{\mathrm{I}}exp\left(i2k_y^{sh}h\right) + T_{21}R_{23}R_{21}R_{23}T_{12}H^{\mathrm{I}}exp\left(i4k_y^{sh}h\right) + \cdots, \tag{32a}$$

$$H^{\mathrm{T}} = T_{23}T_{12}H^{\mathrm{I}}exp\left(ik_y^{sh}h\right) + T_{23}R_{21}R_{23}T_{12}H^{\mathrm{I}}exp\left(i3k_y^{sh}h\right) + T_{23}R_{21}R_{23}R_{21}R_{23}T_{12}H^{\mathrm{I}}exp\left(i5k_y^{sh}h\right) + \cdots, \tag{32b}$$

where H^R,H^T and H^I are the amplitude of reflection, transmission and incident waves, respectively, namely, H_1, H_3 andH_0 in Eq. (27). R_{ij} and T_{ij} are the reflection and transmission coefficients (namely, $H^{\mathrm{R}} = RH^{\mathrm{I}}$ and $H^T = TH^{\mathrm{I}}$) at the interface between medium i and medium j when incident wave is from medium i. k_y^{sh} is the projection of wave vector along y axis. The first term in the right side of Eq. (32a) stands for the first reflection wave at interface 1(between medium 1 and medium 2). The second term stands for the second reflection wave which propagates from the interface 1 to the interface 2 (between medium 2 and medium 3) and is reflected at the interface 2 and then return to the interface 1 and is transmitted at the interface 1. The total phase shift is $\exp(i2k_y^{sh}h)$ during the travel process. Third term stands for the third reflection wave which travels through a slab for two rounds and is eventually transmitted at the interface 1. Each terms in right side of Eq. (32b) can be understand similarly. The first transmission wave propagates through a slab for one way. The second transmission wave propagates through a slab for one round and half and so on. The multiply reflection and transmission process is shown in Fig. 2. After preforming the summation of infinite series, Eq. (35) can be rewritten as

$$H^{\mathrm{R}} = \left(R_{12} + \frac{T_{21}R_{23}T_{12}exp\left(i2k_y^{sh}h\right)}{1 - R_{23}R_{21}exp\left(i2k_y^{sh}h\right)}\right)H^{\mathrm{I}}, \tag{33a}$$

$$H^{\mathrm{T}} = \frac{T_{23}T_{12}exp\left(ik_y^{sh}h\right)}{1 - R_{21}R_{23}exp\left(i2k_y^{sh}h\right)}H^{\mathrm{I}}. \tag{33b}$$

In the case of incident P or incident SV wave, there is mode conversion. The multiply reflection and transmission process is far more complicated and matrix formulation is necessary. Let $\mathbf{a}^{\mathrm{I}} = (A_0,B_0)^T$, $\mathbf{a}^{\mathrm{R}} = (A_1,B_1)^T$ and $\mathbf{a}^{\mathrm{T}} = (A_3,B_3)^T$ stand for the incident waves, the reflection waves and the transmission waves, respectively. $\mathbf{R}_{ij}$ and $\mathbf{T}_{ij}$ are the reflection and transmission matrix ($\mathbf{a}^{\mathrm{R}} = \mathbf{R}\mathbf{a}^{\mathrm{I}}$ and $\mathbf{a}^T = \mathbf{T}\mathbf{a}^{\mathrm{I}}$) of the interface between medium i and medium j when incident wave is from medium i. Then, the resulting reflection and transmission waves can be expressed as

$$\mathbf{a}^{\mathrm{R}} = \mathbf{R}_{12}\mathbf{a}^{\mathrm{I}} + \mathbf{T}_{21}\mathbf{\Lambda}\mathbf{R}_{23}\mathbf{\Lambda}\mathbf{T}_{12}\mathbf{a}^{\mathrm{I}} + \mathbf{T}_{21}\mathbf{\Lambda}\mathbf{R}_{23}\mathbf{\Lambda}\mathbf{R}_{21}\mathbf{\Lambda}\mathbf{R}_{23}\mathbf{\Lambda}\mathbf{T}_{12}\mathbf{a}^{\mathrm{I}} + \cdots, \tag{34a}$$

$$\mathbf{a}^{\mathrm{T}} = \mathbf{T}_{23}\mathbf{\Lambda}\mathbf{T}_{12}\mathbf{a}^{\mathrm{I}} + \mathbf{T}_{23}\mathbf{\Lambda}\mathbf{R}_{21}\mathbf{\Lambda}\mathbf{R}_{23}\mathbf{\Lambda}\mathbf{T}_{12}\mathbf{a}^{\mathrm{I}} + \mathbf{T}_{23}\mathbf{\Lambda}\mathbf{R}_{21}\mathbf{\Lambda}\mathbf{R}_{23}\mathbf{\Lambda}\mathbf{R}_{21}\mathbf{\Lambda}\mathbf{R}_{23}\mathbf{\Lambda}\mathbf{T}_{12}\mathbf{a}^{\mathrm{I}} + \cdots, \tag{34b}$$

where

$$\mathbf{\Lambda} = \begin{pmatrix} exp\left(ik_y^p h\right) & 0 \\ 0 & exp\left(ik_y^s h\right) \end{pmatrix}$$

is the phase shift matrix of waves propagating between the interface 1 and the interface 2. k_y^p and k_y^s are the projections of wave vectors of P wave and SV waves along along y axis, respectively. After preforming the summation of infinite series of matrix, Eq. (34) can be rewritten as

$$\mathbf{a}^{\mathrm{R}} = \left[\mathbf{R}_{12} + \mathbf{T}_{21}(\mathrm{I} - \mathbf{\Lambda}\mathbf{R}_{23}\mathbf{\Lambda}\mathbf{R}_{21})^{-1}\mathbf{\Lambda}\mathbf{R}_{23}\mathbf{\Lambda}\mathbf{T}_{12}\right]\mathbf{a}^{\mathrm{I}}, \tag{35a}$$

$$\mathbf{a}^{\mathrm{T}} = \mathbf{T}_{23}(\mathrm{I} - \mathbf{\Lambda}\mathbf{R}_{21}\mathbf{\Lambda}\mathbf{R}_{23})^{-1}\mathbf{\Lambda}\mathbf{T}_{12}\mathbf{a}^{\mathbf{I}}. \tag{35b}$$

Eqs. (33) and (35) implies that the reflection and transmission coefficients may be a period function of the nondimensional thickness $k_y h$.

4. Energy flux of reflection and transmission and the energy conservation

Energy flux density of a plane wave along the propagation direction $\mathbf{n}$ can be obtained by,

$$q(\mathbf{n},t) = -P_i(\mathbf{n})\dot{u}_i - R_i(\mathbf{n})n_j\dot{u}_{i,j}, \tag{36}$$

where the first term represents the contribution from monopolar tractions and second term the contribution from dipolar tractions. Due to the time dependence of energy flux, the average energy flux over one period, namely, $\overline{q}(\mathbf{n}) = \frac{1}{T}\int_0^T q(\mathbf{n},t)dt$ is more interesting and can be calculated by

$$\overline{q}_0^p = \frac{1}{2}\omega\sigma_{p1}^3\left[(\lambda_1 + 2\mu_1) - \mu_1 m_1 + 2c_1(\lambda_1 + 2\mu_1)\sigma_{p1}^2\right]A_0A_0^* \tag{37a}$$

$$\overline{q}_0^s = \frac{1}{2}\omega\sigma_{s1}^3\mu_1\left(1 - m_1 + 2c_1\sigma_{s1}^2\right)B_0B_0^* \tag{37b}$$

$$\overline{q}_0^{sh} = \frac{1}{2}\omega\sigma_{sh1}\mu_1\left(1 - m_1 + 2c_1\sigma_{sh1}^2\right)H_0H_0^* \tag{37c}$$

for incident P wave, SV wave and SH wave, respectively.

$$\overline{q}_i^p = \frac{1}{2}\omega\sigma_{pi}^3\left[(\lambda_i + 2\mu_i) - \mu_i m_i + 2c_i(\lambda_i + 2\mu_i)\sigma_{pi}^2\right]A_iA_i^*\ (i = 1,3) \tag{38a}$$

$$\overline{q}_i^s = \frac{1}{2}\omega\sigma_{si}^3\mu_i\left(1 - m_i + 2c_i\sigma_{si}^2\right)B_iB_i^* \tag{38b}$$

$$\overline{q}_i^{sh} = \frac{1}{2}\omega\sigma_{shi}\mu_i\left(1 - m_i + 2c_i\sigma_{shi}^2\right)H_iH_i^* \tag{38c}$$

for reflection waves ($i = 1$) and transmission waves ($i = 3$).

$$\overline{q}_2^{p^\pm} = \frac{1}{2}\omega\sigma_{p2}^3\left[(\lambda_2 + 2\mu_2) - \mu_2 m_2 + 2c_2(\lambda_2 + 2\mu_2)\sigma_{p2}^2\right]A_2^\pm A_2^{\pm *}, \tag{39a}$$

$$\overline{q}_2^{s^\pm} = \frac{1}{2}\omega\sigma_{s2}^3\mu_2\left(1 - m_2 + 2c_2\sigma_{s2}^2\right)B_2^\pm B_2^{\pm *}, \tag{39b}$$

$$\overline{q}_2^{sh^\pm} = \frac{1}{2}\omega\sigma_{sh2}\mu_2\left(1 - m_2 + 2c_2\sigma_{sh2}^2\right)H_2^\pm H_2^{\pm *}, \tag{39c}$$

for the forward and the backward propagating waves in the slab. In Eqs. (37)–(39), $\lambda_i + 2\mu_i = \frac{2(1-\nu_i)}{1-2\nu_i}\mu_i$. Symbol * indicates the complex conjugate quantity.

For the SP and SS surface waves, because the displacement distribution on the wavefront of surface waves is not homogeneous, the value of energy flux density on the wavefront is thus position-dependent and decreases gradually with the increase of $|y|$. Here, a unit area is taken to be $l_z \times l_y = \gamma_p \times 1/\gamma_p$ or $l_z \times l_y = \gamma_s \times 1/\gamma_s$ near the surface, Then, the energy fluxes through the prescribed unit area are

$$\overline{q}_i^{sp} = \frac{1}{2}M\omega\xi_i\left(C_iC_i^*\right)J_i^{sp}\exp(\pm 2n\gamma_{pi}h), \tag{40a}$$

$$\overline{q}_i^{ss} = \frac{1}{2}M\omega\xi_i\left(D_iD_i^*\right)J_i^{ss}\exp(\pm 2n\gamma_{si}h), \tag{40b}$$

$$\overline{q}_i^{sh} = \frac{1}{2}M\omega\zeta_{shi}\left(F_iF_i^*\right)J_i^{sh}\exp(\pm 2n\gamma_{shi}h), \tag{40c}$$

where $n = 0$ for the surface waves at interface between medium 1 and medium 2; $n = 1$ for the surface wave at interface between medium 2 and medium 3; Eq. (40) takes the plus sign when $i = 2$ and the minus sign when $i = 3$. Besides,

$$M = \frac{1 - \exp(-2)}{2},$$

$$J_i^{sp} = \lambda_i\tau_{pi}^2 - 2\mu_i\left(\tau_{pi}^2 + \xi_i^2\right) + \mu_i m_i\left(\tau_{pi}^2 + 2\xi_i^2\right) + 2c_i\tau_{pi}^2\left[\lambda_i\xi_i^2 + 2\mu_i\left(\tau_{pi}^2 + 2\xi_i^2\right)\right],$$

$$J_i^{ss} = \mu_i\left[-\left(3\tau_{si}^2 + 4\xi_i^2\right) + m_i\left(\tau_{si}^2 + 2\xi_i^2\right) + 2c_i\tau_{si}^2\left(2\tau_{si}^2 + 3\xi_i^2\right)\right].$$

$$J_i^{sh} = \mu_i\left(m_i - 1 + 2c_i\tau_{shi}^2\right).$$

Define the reflection and transmission coefficients as the energy flux ratios along the propagation directions of various reflection waves and transmission waves with respect to incident waves, namely, $\overline{q}_1^p(\mathbf{n}_{P1})/\overline{q}_0^p(\mathbf{n}_0)$, $\overline{q}_1^s(\mathbf{n}_{s1})/\overline{q}_0^p(\mathbf{n}_0)$, $\overline{q}_1^{sp}(\mathbf{n})/\overline{q}_0^p(\mathbf{n}_0)$ and $\overline{q}_1^{ss}(\mathbf{n})/\overline{q}_0^p(\mathbf{n}_0)$ for the reflection coefficients, $\overline{q}_3^p(\mathbf{n}_{P3})/\overline{q}_0^p(\mathbf{n}_0)$, $\overline{q}_3^s(\mathbf{n}_{s3})/\overline{q}_0^p(\mathbf{n}_0)$, $\overline{q}_3^{sp}(\mathbf{n})/\overline{q}_0^p(\mathbf{n}_0)$ and $\overline{q}_3^{ss}(\mathbf{n})/\overline{q}_0^p(\mathbf{n}_0)$ for the transmission coefficients and $\overline{q}_2^{p^\pm}(\mathbf{n}_{p^\pm})/\overline{q}_0^p(\mathbf{n}_0)$, $\overline{q}_2^{s^\pm}(\mathbf{n}_{s^\pm})/\overline{q}_0^p(\mathbf{n}_0)$, $\overline{q}_2^{sp^\pm}(\mathbf{n}_{sp^\pm})(\mathbf{n})/\overline{q}_0^p(\mathbf{n}_0)$ and $\overline{q}_2^{ss^\pm}(\mathbf{n}_{ss^\pm})/\overline{q}_0^p(\mathbf{n}_0)$ for the coefficients of forward and backward waves in the medium 2 in the case of incident P wave. In the case of incident SH wave, $\overline{q}_1^{sh}(\mathbf{n}_{sh1})/\overline{q}_0^{sh}(\mathbf{n}_0)$, and $\overline{q}_1^{ssh}(\mathbf{n})/\overline{q}_0^{sh}(\mathbf{n}_0)$ for the reflection coefficients, $\overline{q}_3^{sh}(\mathbf{n}_{sh3})/\overline{q}_0^{sh}(\mathbf{n}_0)$, and $\overline{q}_3^{ssh}(\mathbf{n})/\overline{q}_0^{sh}(\mathbf{n}_0)$ for the transmission coefficients and $\overline{q}_2^{sh^\pm}(\mathbf{n}_{sh^\pm})/\overline{q}_0^{sh}(\mathbf{n}_0)$ and $\overline{q}_2^{ssh^\pm}(\mathbf{n})/\overline{q}_0^{sh}(\mathbf{n}_0)$ for the coefficients of forward and backward waves in the medium 2. Consider that the energy flux vectors of various surface waves are along the interface, the energy conservation requires that the normal input energy flux is equal to the normal output energy flux through a thin layer with an infinitesimal thickness at $y = 0$, namely,

$$E_1 = \frac{\overline{q}_1^p\cos\theta_1 + \overline{q}_1^s\cos\theta_2 + \overline{q}_2^{p^+}\cos\theta_p + \overline{q}_2^{s^+}\cos\theta_s - \overline{q}_2^{p^-}\cos\theta_p - \overline{q}_2^{s^-}\cos\theta_s}{\overline{q}_0^p\cos\theta_1} = 1 \tag{41}$$

Similarly, the energy conservation through a thin layer at $y = h$ requires

$$E_2 = \frac{-\overline{q}_2^{p^+}\cos\theta_p - \overline{q}_2^{s^+}\cos\theta_s + \overline{q}_2^{p^-}\cos\theta_p + \overline{q}_2^{s^-}\cos\theta_s + \overline{q}_3^p\cos\theta_3 + \overline{q}_3^s\cos\theta_4}{\overline{q}_0^p\cos\theta_1} = 0 \tag{42}$$

Combining Eqs. (41) and (42) leads to

$$E = E_1 + E_2 = \frac{\overline{q}_1^p\cos\theta_1 + \overline{q}_1^s\cos\theta_2 + \overline{q}_3^p\cos\theta_3 + \overline{q}_3^s\cos\theta_4}{\overline{q}_0^p\cos\theta_1} = 1 \tag{43}$$

for the incident P wave. In the case of incident SH wave, Eq. (44) is replaced by

$$E = E_1 + E_2 = \frac{\overline{q}_1^{sh}\cos\theta_1 + \overline{q}_3^{sh}\cos\theta_3}{\overline{q}_0^{sh}\cos\theta_1} = 1 \tag{44}$$

Eqs. (43) and (44) mean that the normal input energy flux is equal to the normal output energy flux through a slab with a finite

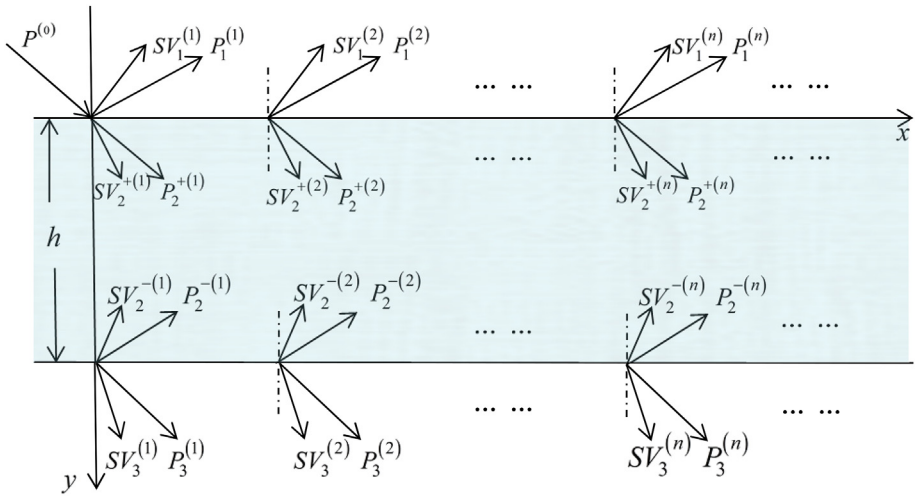

Fig. 2. Sketch of multiply reflection and transmission of bulk waves.

thickness when no energy is absorbed and created in the slab and can be used to validate the numerical results.

5. Numerical examples and discussion

In the numerical examples, the main concerns are focused on the influences of the microstructure parameter c and d, and the thickness h of slab on the reflection and transmission coefficients. The Poisson's ratio of medium 1 and medium 2 is taken to be $\nu_1 = \nu_2 = 1/3$. The density ratio and the shear modulus ratio of them are assumed to be $\overline{\rho}(= \rho_1/\rho_2) = 1.2$ and $\overline{\mu}(= \mu_1/\mu_2) = 1.8$, respectively. Two half-spaces characteristic of the classical elasticity and the gradient elasticity are both considered. The reflection and transmission coefficients in terms of energy flux ratio in two cases of incident waves, namely, in-plane P wave and the out-of-plane SH wave, are both calculated.

5.1. Incident P wave case

Fig. 3 shows the dependence of reflection and transmission coefficients on the nondimensional thickness h/λ in the case of elastic half-spaces and incident longitudinal wave. It is observed that the reflection and transmission coefficients are all the periodic function of the nondimensional thickness h/λ. At certain thickness, the reflection P wave or SV wave may disappear, and the transmissions waves reach their peak values. But the transmission P wave and transmission SV wave cannot reach their peaks at same time, in general. Moreover, the fluctuant periods of reflection and transmission coefficients are different for longitudinal wave and transverse wave and are dependent of the incident angles. These observations are consistent with Eqs. (36) and (38) obtained from the multiple reflection/transmission approach. It is also noted that the transmission P wave is always nonzero but the transmission SV wave maybe zero at certain thickness in the case of incident P wave. On the other hand, Fig. 3 can be understood the dependence of reflection and transmission coefficients on the incident wavelength for a fixed thickness of slab. The periodical fluctuant phenomena reflect the selective nature of the sandwich structure to incident waves. These observations mean that the sandwich structure can be used as a filter.

Fig. 4 shows the dependence of reflection and transmission coefficients on the nondimensional wavelength $\overline{\lambda} = \lambda/d$ in the case of elastic half-spaces and incident P wave. It is observed that the reflection and transmission coefficients are asymptotic to that of classic elastic slab with the increasing of incident wavelength. This means that the effects of microstructure are evident only when the incident wavelength is comparable to the characteristic length of microstructure and can be ignored when the incident wavelength is far larger than the microstructure length. These observations are completely consistent with that reported by Gourgiotis et al. (2013). Moreover, it is observed that the reflection coefficients of both P wave and SV wave decrease when the nondimensional wavelength increases. This means that the incident wave with longer wavelength can propagate through the slab easier. Compared with the reflection coefficients obtained by Gourgiotis et al. (2013) for the free surface (see Fig. 2 in Gourgiotis et al. (2013)), the reflection of P wave always weaken when the incident wavelength increases. However, the reflection of SV wave weaken in the slab situation while reinforce in the free surface situation. This difference can be understood by considering the restriction of energy conservation in the free surface situation.

Fig. 5 shows the dependence of reflection and transmission on the microstructure parameter $\alpha_2 = \sqrt{c_2}/d_2$ in the case of elastic half-spaces and incident P wave. It is observed that the reflection and transmission SV wave are suppressed with the increasing of microstructure parameter α_2. In other word, the increasing of microstructure parameter α_2 does not help to the mode conversion. It is also noted that the transmission P wave increases while the reflection P wave decreases as the microstructure parameter α_2 increasing. This implies that the larger microstructure parameter α_2 makes the incident P wave propagating through a gradient elastic slab more easily. Moreover, the influences of microstructure parameter α_2 are more evident on the surface waves in the gradient elastic slab than on the bulk waves. The amplitudes of surface waves increase monotonously as the microstructure parameter $\overline{\alpha}$ increasing. By compared with numerical results obtained by Gourgiotis et al. (2013) for the free surface (see Fig. 4 in Gourgiotis et al. (2013)), a similar phenomenon is observed, namely, the increase of the microstructure parameter α_2 results in the decrease of reflection of P wave.

From the numerical results obtained from a gradient elastic slab sandwiched by two classic elastic half-spaces, the influences of the microstructure parameter of slab on the reflection and transmission waves can be discussed. In order to further study the influences of microstructure parameter ratio, the reflection and transmission coefficients through a slab sandwiched by two gradient elastic half-spaces are also calculated. Fig. 6 shows the dependence of reflection and transmission on the microstructure

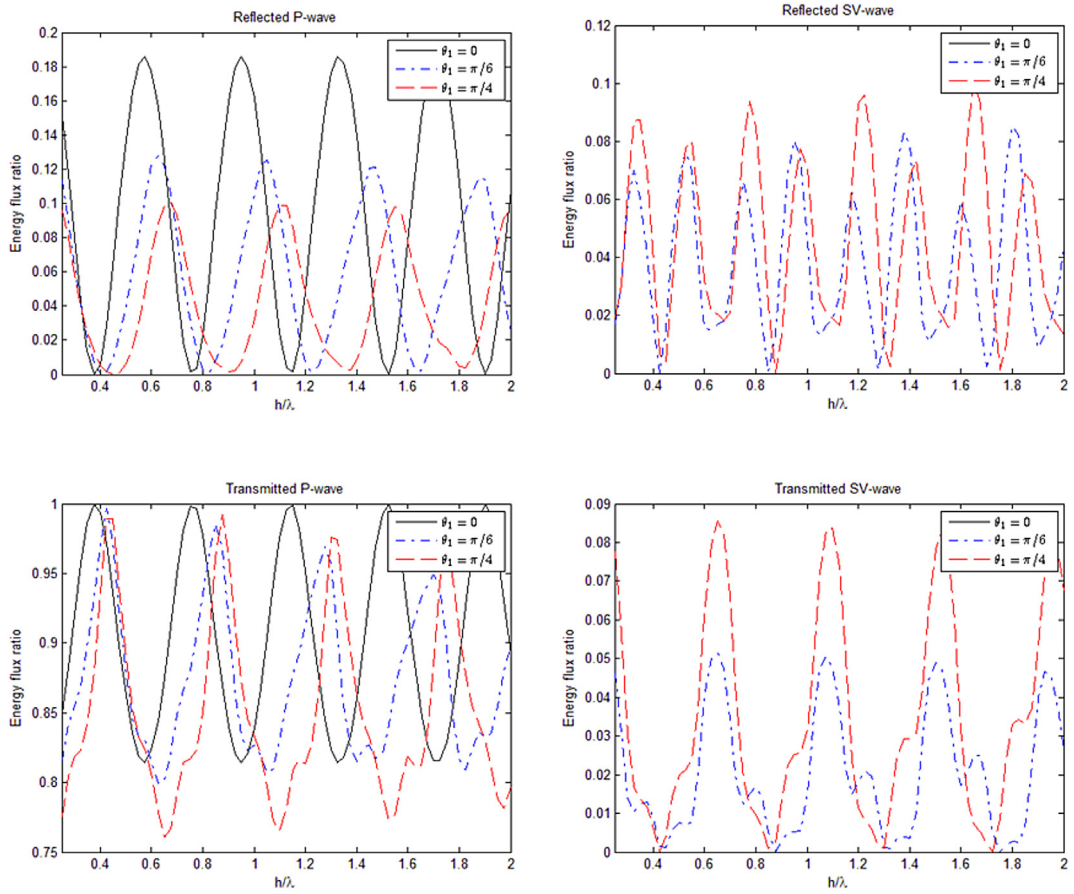

Fig. 3. The dependence of reflection and transmission on the dimensional thickness h/λ in the case of elastic half-spaces and incident Longitudinal wave ($\alpha_2 = 1$, $\overline{\lambda} = 10$).

parameter ratio $\overline{d} = d_1/d_2$ in the case of incident P wave. It is observed that the reflection and transmission SV waves are more sensitive to the microstructure parameter ratio $\overline{d}$ than the reflection and transmission P waves. The increasing of the microstructure parameter ratio $\overline{d}$ makes the reflection SV wave increasing while the transmission SV wave decreasing. The influence on the P wave is opposite to the influences on the SV wave. However, the microstructure parameter ratio $\overline{d}$ has same influences on both SP type and SS type surface waves. The increasing of the microstructure parameter ratio $\overline{d}$ makes the reflection and transmission surface waves, both of SP type and SS type, decreasing monotonously.

5.2. Incident SH wave case

Fig. 7 shows the dependence of reflection and transmission coefficients in two elastic half-spaces on the nondimensional wavelength $\overline{\lambda} = \lambda/d_2$. Similar to the incident P wave case, the reflection and transmission coefficients are asymptotic to that of elastic slab as the incident wavelength increasing. The microstructure effects cannot be ignored only when the incident wavelength is comparable to the microstructure length.

Fig. 8 shows the dependence of reflection and transmission coefficients in two elastic half-spaces on the nondimensional thickness h/λ. The periodic dependence of reflection and transmission coefficients on the thickness of slab is also observed as in the case of incident P wave. The periodical dependences on the thickness of slab can be explained by the constructive and destructive interfering among the multiple reflection waves (transmission waves). The phase shift among the multiple reflection waves (transmission waves) is $exp(ink_y h)$ which result in the periodical dependence of reflection and transmission coefficients on the thickness of slab or the incident wavelength. The periodic dependence of reflection and transmission P and SV waves on the thickness of slab can be explained similarly.

Fig. 9 show the dependence of reflection and transmission coefficients on the microstructure parameter $\alpha_2 = \sqrt{c_2}/d_2$ in the case of two elastic half-spaces. It is observed that the increasing of the microstructure parameter α_2 makes the reflection coefficient decreasing and the transmission coefficient increasing. It is also noted that there is a critical angle $\theta_{cr} \approx 60^\circ$ where the reflection SH wave disappears and the total transmission phenomenon takes place.

Fig. 10 shows the dependence of reflection and transmission coefficients on the microstructure parameter ratio $\overline{d} = d_1/d_2$ in the case of two gradient elastic half-spaces. It is observed that the reflection and transmission surface waves (SSH) are more sensitive to the microstructure parameter ratio $\overline{d}$ than the reflection and transmission bulk waves and decrease monotonously with the increasing of $\overline{d}$ as in the case of incident P wave. However, the influences of $\overline{d}$ on the reflection bulk wave and transmission bulk wave are opposite, namely, the reflection bulk wave decreasing while the transmission bulk wave increasing as the microstructure parameter ratio $\overline{d}$ increasing. This means that the larger microstructure parameter $\overline{d}$ makes the SH wave propagating through the slab more easy.

5.3. Verification of energy conservation

The reflection and transmission coefficients are defined by the energy flux ratio of reflection and transmission waves with respect

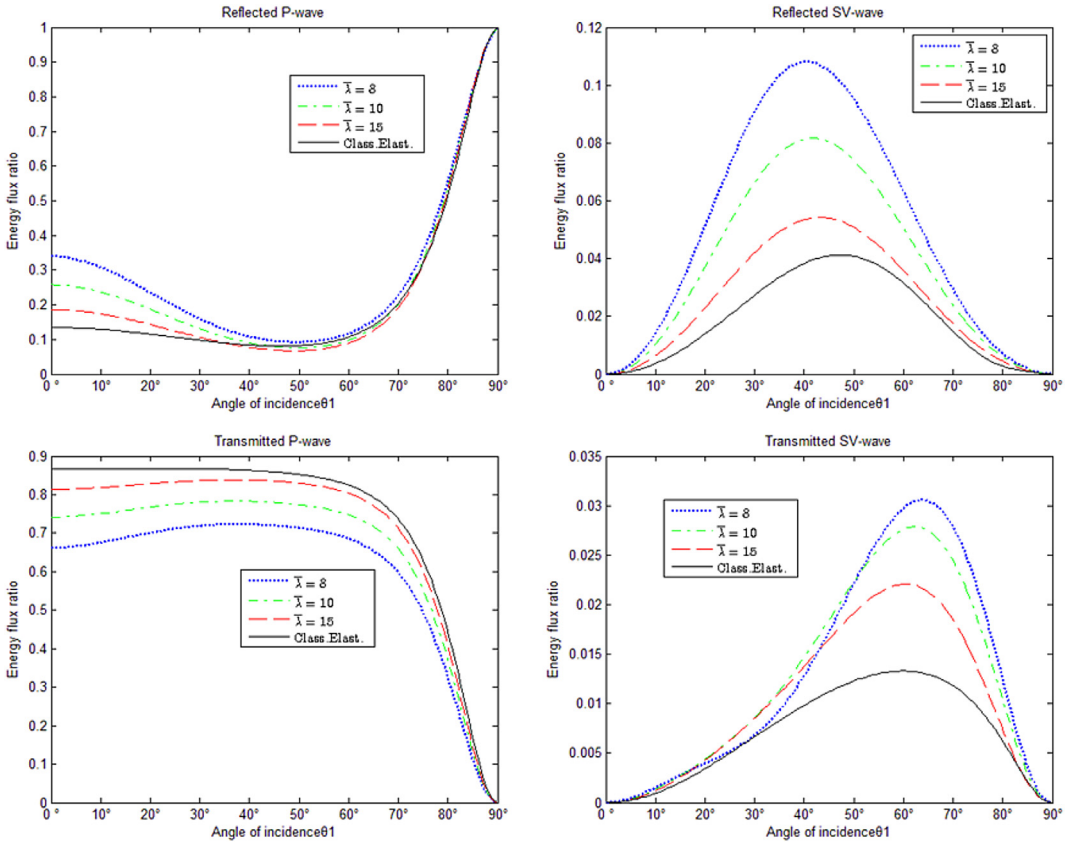

Fig. 4. The dependence of reflection and transmission on the nondimensional wavelength $\bar{\lambda} = \lambda/d_2$ in the case of elastic half-spaces and incident Longitudinal wave ($\alpha_2 = 0.1$, $\bar{h} = 0.2$).

to the incident wave in present work. The advantage of such definition is that the energy conservation can be easily checked and thus facilitates the validation of the numerical results. Fig. 11 shows energy conservation curves at different incident wavelength in the case of incident P wave and SH wave, respectively, for a slab sandwiched by two gradient elastic half-spaces. It is observed that energy conservation is satisfied approximately with an acceptable error in total range of incident angles. The numerical error is maximal at normal incident case and decrease gradually as the incident angle increasing.

6. Conclusions

When the elastic waves propagate through a slab sandwiched by two elastic or gradient elastic half-spaces, the reflection and transmission problem is far more complicated than the reflection and transmission at bi-materials interface. There are two interfaces and three characteristic lengths, namely, the incident wavelength, the geometrical thickness of slab and the microstructure length of gradient elastic solid. The dependence of reflection and transmission waves on these characteristic lengths and the microstructure parameters of slab are main concerns of present work. The reflection and transmission coefficients in terms of energy flux ratio are calculated for a gradient elastic slab under an incident P wave or an incident SH wave. From the numerical results, the following conclusions can be drawn.

1) The reflection and transmission coefficients are the periodical function of the thickness of slab for an incident wave with fixed wavelength. At certain specific thickness, the reflection SH wave, reflection P wave or reflection SV wave may disappear. But the reflection P wave and the reflection SV wave cannot disappear at same time. For a slab with fixed thickness, the reflection and transmission coefficients are also periodical functions of the incident wavelength. Some incident waves with certain frequency can propagate through the slab easily while other of incident waves cannot. The selective nature of the slab to the incident waves makes the sandwiched structure a frequency filter.
2) The microstructure parameters have more evident influences on the surface waves than on the bulk waves. The amplitude of surface waves, including SP type, SS type and SSH type, increase monotonously as the microstructure parameter increasing. Moreover, in the case of incident P wave, the microstructure effects do not help the mode conversion.
3) The microstructure effects make the bulk waves dispersive and the surface waves appearing. The reflection and transmission coefficients of bulk waves through a gradient elastic slab thus deviate from that of classic elastic slab. The deviation cannot be ignored only when the incident wavelength is comparable to the microstructure length and decreases gradually as the incident wavelength increasing. In other word, the reflection and transmission coefficients are asymptotic to that of classic elastic slab as the incident wavelength increasing.
4) The microstructure characteristic length ratio of the half-space to that of slab has more evident influence on the SV wave than on the P wave. In general, the reflection coefficient increases while the transmission coefficient decreases for SV wave

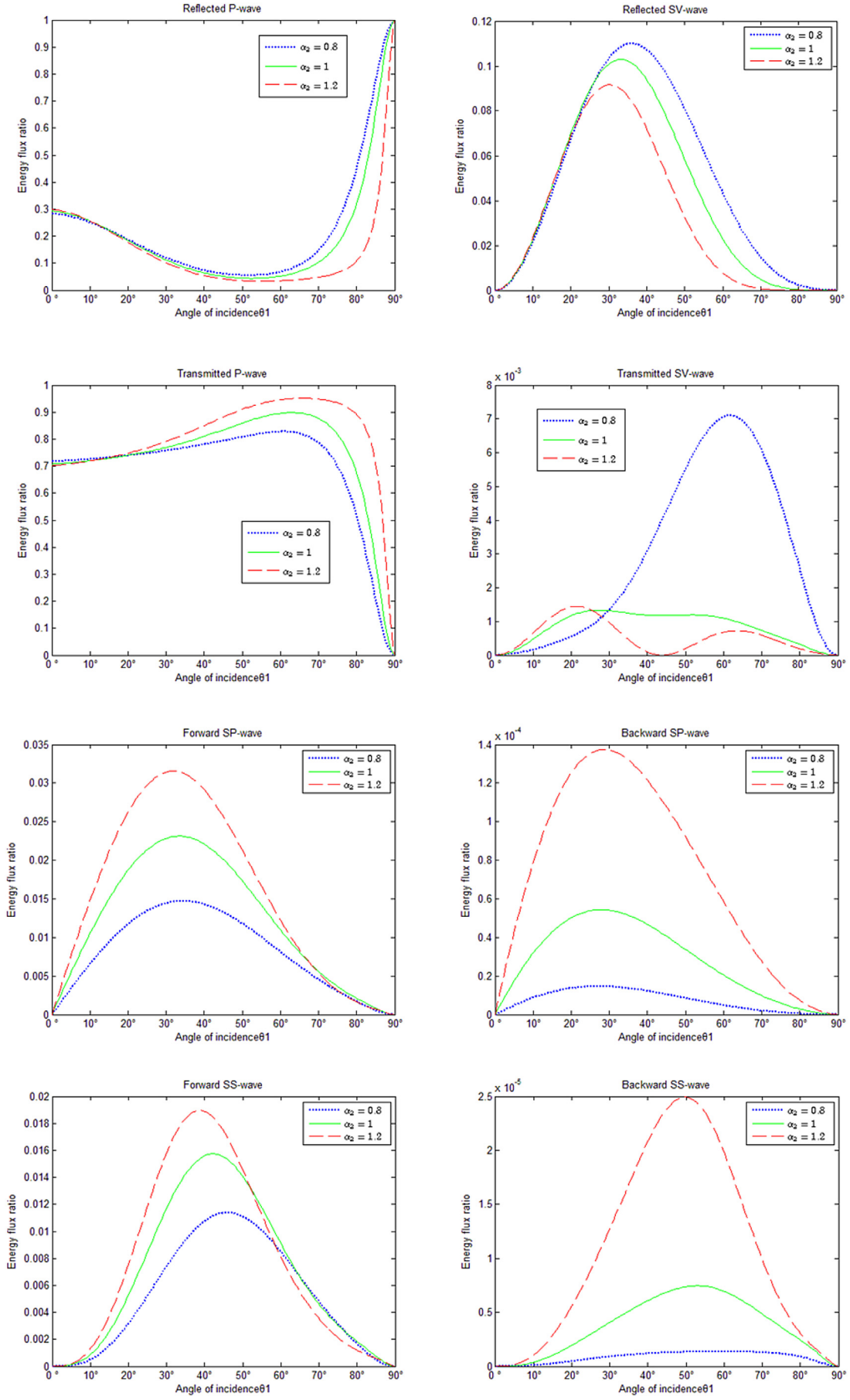

Fig. 5. The dependence of reflection and transmission on the microstructure parameter $\alpha_2 = \sqrt{c_2}/d_2$ in the case of elastic half-spaces and incident Longitudinal wave ($\overline{\lambda} = 10$, $\overline{h} = 0.2$).

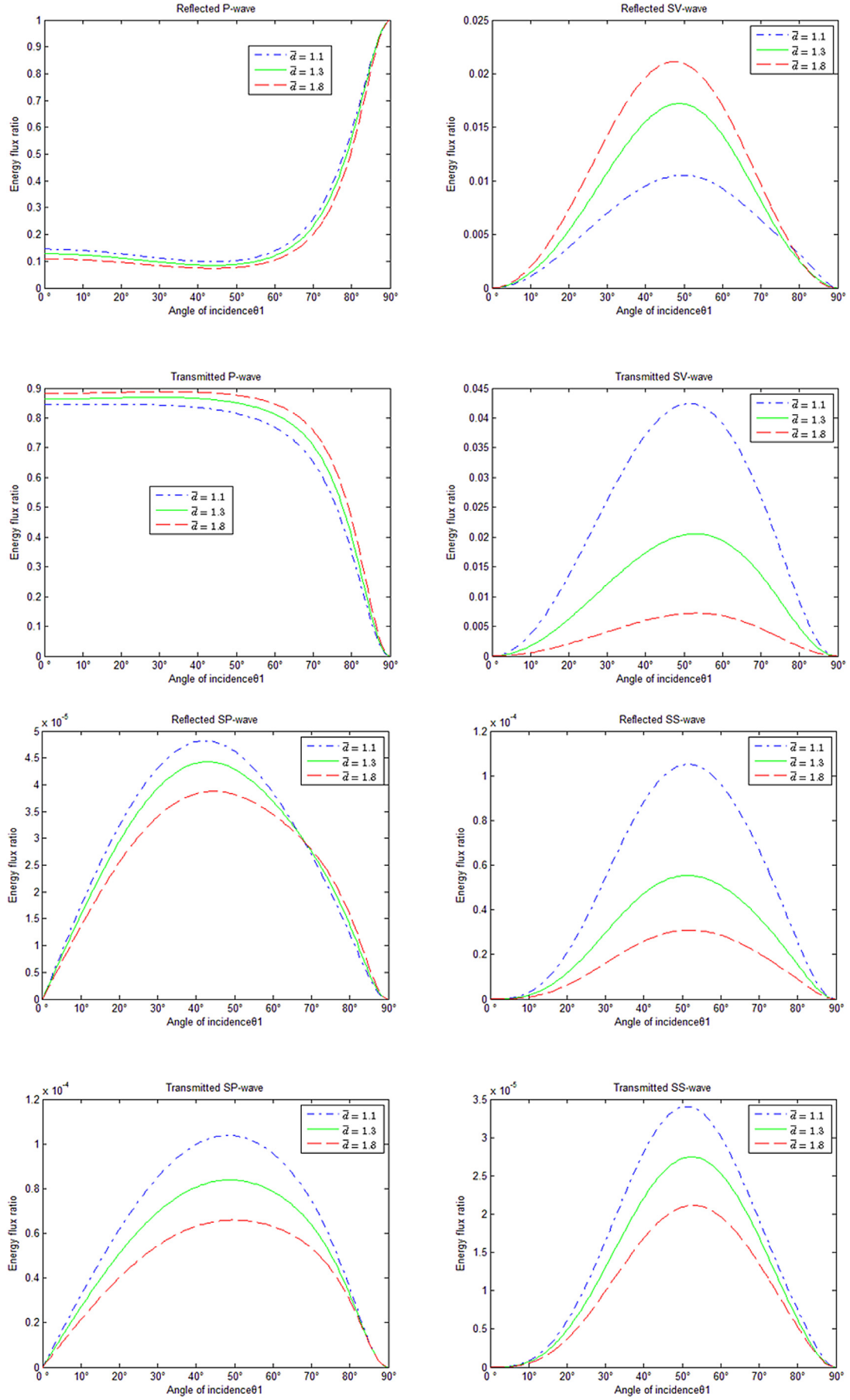

Fig. 6. The dependence of reflection and transmission on the microstructure parameter ratio $\overline{d} = d_1/d_2$ in the case of gradient elastic half-spaces and incident P wave ($\alpha_1 = 0.1$, $\overline{\lambda} = 10$, $\overline{h} = 0.2$, $\overline{c} = c_1/c_2 = 1.1$).

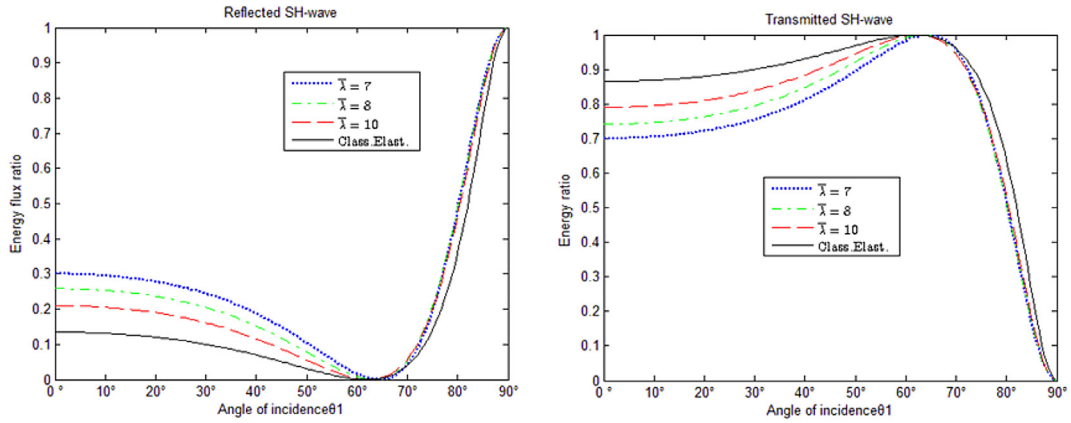

Fig. 7. The dependence of reflection and transmission on the nondimensional wavelength $\overline{\lambda} = \lambda/d_2$ in the case of elastic half-spaces and incident SH wave ($\alpha_2 = 0.1$, $\overline{h} = 0.2$).

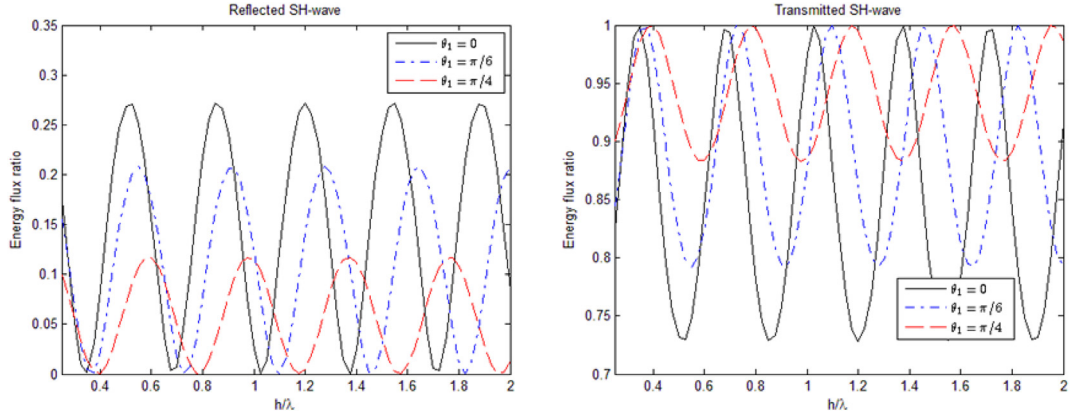

Fig. 8. The dependence of reflection and transmission on the dimensional thickness h/λ in the case of elastic half-spaces and incident SH wave ($\alpha_2 = 0.1$, $\overline{\lambda} = 8$).

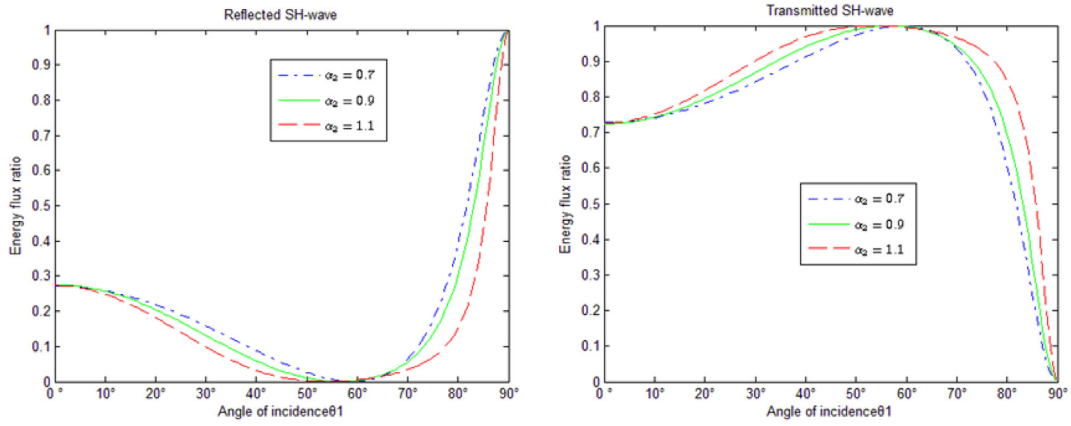

Fig. 9. The dependence of reflection and transmission on the microstructure parameter $\alpha_2 = \sqrt{c_2}/d_2$ in the case of elastic half-spaces and incident SH wave ($\overline{\lambda} = 7$, $\overline{h} = 0.2$).

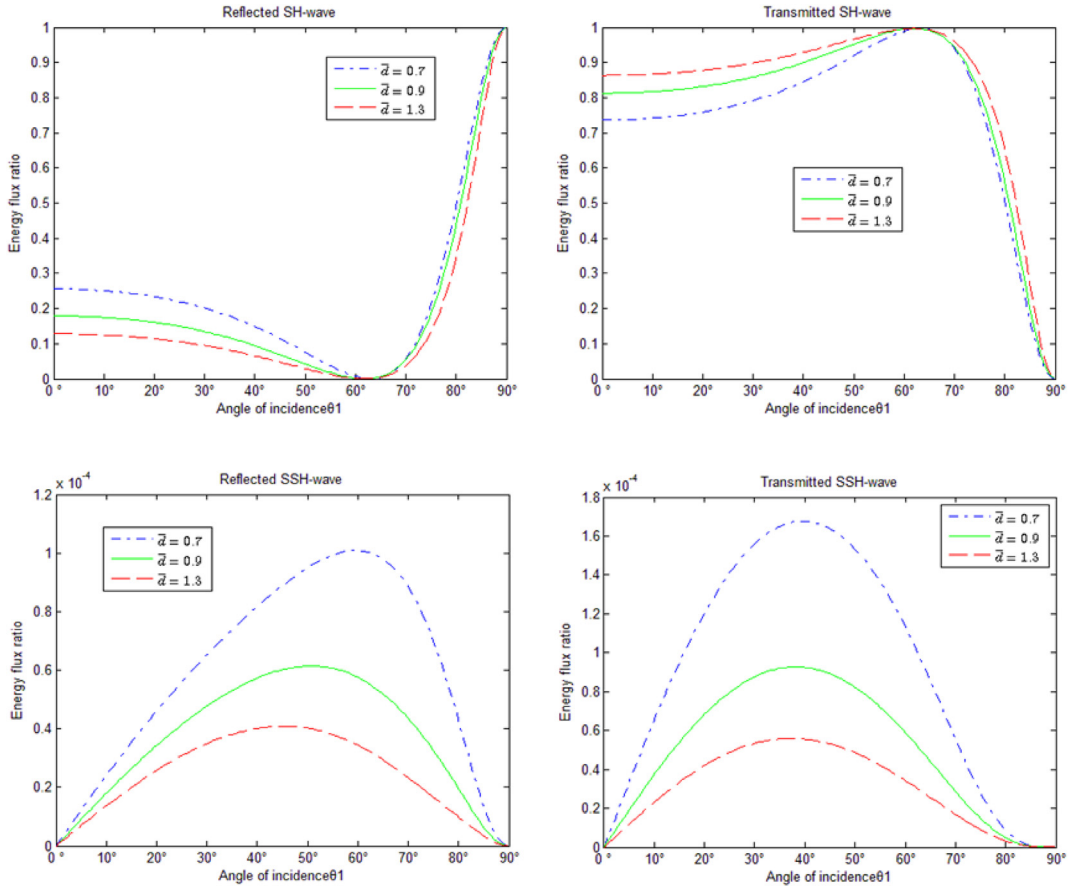

Fig. 10. The dependence of reflection and transmission on the microstructure parameter ratio $\overline{d} = d_1/d_2$ in the case of gradient elastic half-spaces and incident SH wave ($\alpha_1 = 0.1$, $\overline{\lambda} = 10$, $\overline{h} = 0.2$, $\overline{c} = c_1/c_2 = 1.1$).

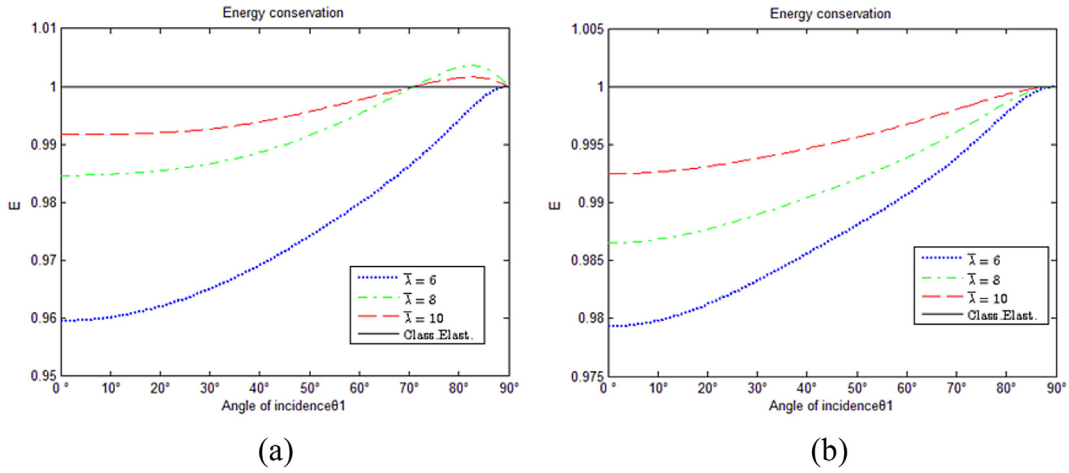

Fig. 11. Validation of energy conservation in the case of incident P wave and SH wave for a slab sandwiched by two gradient elastic half-spaces. (a) for incident P wave($\alpha_2 = 0.1$, $\overline{h} = 0.2$); (b) for incident SH wave ($\alpha_2 = 0.1$, $\overline{h} = 0.2$).

as the characteristic length ratio increasing. The changes of the reflection coefficients and transmission coefficient of P wave and SH wave are opposite to that of SV waves. In contrast, the reflection and transmission surface waves are more sensitive to the characteristic length ratio and decrease monotonously as the characteristic length ratio increasing.

Acknowledgement

The work is supported by Fundamental Research Funds for the Central Universities (FRF-BR-15-026A) and the National Natural Science Foundation of China (No. 10972029) and Opening fund of State Key Laboratory of Nonlinear Mechanics (LNM).

Appendix A

The explicit expression of matrix $\mathbf{A}=(a_{i,j})_{16\times16}$ and $\mathbf{B}=(b_{i,j})_{16\times1}$ in Eq. (28) are given here when the medium 1, medium 2 and medium 3 are all dipolar gradient elasticity. The counterpart when the medium 1 and medium 3 are the classical elasticity is not given for brevity but can be obtained from the present formulation by corresponding modification. Moreover, the explicit expression of matrix **A** and **B** for incident SH wave are also not provided here for brevity.

$$a_{1,1}=a_{1,2}=\xi_1,\ a_{1,3}=-\beta_{s1},\ a_{1,4}=-i\gamma_{s1},\ a_{1,5}=a_{1,6}=a_{1,7}=a_{1,8}=-\xi_2,\ -a_{1,9}=a_{1,11}=\beta_{s2},$$

$$-a_{1,10}=a_{1,12}=i\gamma_{s2},\ a_{2,1}=-\beta_{p1},\ a_{2,2}=-i\gamma_{p1},\ a_{2,3}=a_{2,4}=-\zeta_1,\ -a_{2,5}=a_{2,7}=\beta_{p2},$$

$$-a_{2,6}=a_{2,8}=i\gamma_{p2},\ a_{2,9}=a_{2,10}=a_{2,11}=a_{2,12}=\zeta_2,\ a_{3,1}=\xi_1\beta_{p1},\ a_{3,2}=i\xi_1\gamma_{p1},\ a_{3,3}=-\beta_{s1}^2,$$

$$a_{3,4}=\gamma_{s1}^2,\ a_{3,5}=-a_{3,7}=\xi_2\beta_{p2},\ a_{3,6}=-a_{3,8}=i\xi_2\gamma_{p2},\ a_{3,9}=a_{3,11}=\beta_{s2}^2,\ a_{3,10}=a_{3,12}=-\gamma_{s2}^2,$$

$$a_{4,1}=-\beta_{p1}^2,\ a_{4,2}=\gamma_{p1}^2,\ a_{4,3}=-\zeta_1\beta_{s1},\ a_{4,4}=-i\zeta_1\gamma_{s1},\ a_{4,5}=a_{4,7}=\beta_{p2}^2,\ a_{4,6}=a_{4,8}=-\gamma_{p2}^2,$$

$$-a_{4,9}=a_{4,11}=\zeta_2\beta_{s2},\ -a_{4,10}=a_{4,12}=i\zeta_2\gamma_{s2},$$

$$a_{5,1}=\mu_1\Big[2\xi_1\beta_{p1}+2c_1\xi_1\beta_{p1}\Big(2\sigma_{p1}^2+\xi_1^2\Big)-m_1\xi_1\beta_{p1}\Big],$$

$$a_{5,2}=\mu_1\Big[2\xi_1\gamma_{p1}i-2c_1\xi_1\gamma_{p1}\Big(2\tau_{p1}^2-\xi_1^2\Big)i-m_1\xi_1\gamma_{p1}i\Big],$$

$$a_{5,3}=\mu_1\Big[\Big(\zeta_1^2-\beta_{s1}^2\Big)-c_1\Big(\beta_{s1}^4-\zeta_1^4+2\zeta_1^2\beta_{s1}^2\Big)+m_1\beta_{s1}^2\Big],$$

$$a_{5,4}=\mu_1\Big[\Big(\zeta_1^2+\gamma_{s1}^2\Big)-c_1\Big(\gamma_{s1}^4-\zeta_1^4-2\zeta_1^2\gamma_{s1}^2\Big)-m_1\gamma_{s1}^2\Big],$$

$$a_{5,5}=-\mu_2\Big[-2\xi_2\beta_{p2}-2c_2\xi_2\beta_{p2}\Big(2\sigma_{p2}^2+\xi_2^2\Big)+m_2\xi_2\beta_{p2}\Big],$$

$$a_{5,6}=-\mu_2\Big[-2\xi_2\gamma_{p2}i+2c_2\xi_2\gamma_{p2}\Big(2\tau_{p2}^2-\xi_2^2\Big)i+m_2\xi_2\gamma_{p2}i\Big],$$

$$a_{5,7}=-\mu_2\Big[2\xi_2\beta_{p2}+2c_2\xi_2\beta_{p2}\Big(2\sigma_{p2}^2+\xi_2^2\Big)-m_2\xi_2\beta_{p2}\Big],$$

$$a_{5,8}=-\mu_2\Big[2\xi_2\gamma_{p2}i-2c_2\xi_2\gamma_{p2}\Big(2\tau_{p2}^2-\xi_2^2\Big)i-m_2\xi_2\gamma_{p2}i\Big],$$

$$a_{5,9}=-\mu_2\Big[\Big(\zeta_2^2-\beta_{s2}^2\Big)-c_2\Big(\beta_{s2}^4-\zeta_2^4+2\zeta_2^2\beta_{s2}^2\Big)+m_2\beta_{s2}^2\Big],$$

$$a_{5,10}=-\mu_2\Big[\Big(\zeta_2^2+\gamma_{s2}^2\Big)-c_2\Big(\gamma_{s2}^4-\zeta_2^4-2\zeta_2^2\gamma_{s2}^2\Big)-m_2\gamma_{s2}^2\Big],$$

$$a_{5,11}=-\mu_2\Big[\Big(\zeta_2^2-\beta_{s2}^2\Big)-c_2\Big(\beta_{s2}^4-\zeta_2^4+2\zeta_2^2\beta_{s2}^2\Big)+m_2\beta_{s2}^2\Big],$$

$$a_{5,12}=-\mu_2\Big[\Big(\zeta_2^2+\gamma_{s2}^2\Big)-c_2\Big(\gamma_{s2}^4-\zeta_2^4-2\zeta_2^2\gamma_{s2}^2\Big)-m_2\gamma_{s2}^2\Big],$$

$$a_{6,1}=\mu_1\Big[-2\Big(\sigma_{p1}^2+\beta_{p1}^2\Big)-2c_1\Big(\xi_1^4+4\xi_1^2\beta_{p1}^2+2\beta_{p1}^4\Big)+m_1\beta_{p1}^2\Big],$$

$$a_{6,2}=\mu_1\Big[2\Big(2\tau_{p1}^2+\xi_{p1}^2\Big)-2c_1\Big(\xi_1^4-4\xi_1^2\gamma_{p1}^2+2\gamma_{p1}^4\Big)-m_1\gamma_{p1}^2\Big],$$

$$a_{6,3}=\mu_1\Big[-2\zeta_1\beta_{s1}-c_1\zeta_1\beta_{s1}\Big(\sigma_{s1}^2+2\zeta_1^2\Big)+m_1\zeta_1\beta_{s1}\Big],$$

$$a_{6,4}=\mu_1\Big[-2\zeta_1\gamma_{s1}i+c_1\zeta_1\gamma_{s1}\Big(\tau_{s1}^2-2\zeta_1^2\Big)i+m_1\zeta_1\gamma_{s1}i\Big],$$

$$a_{6,5}=-\mu_2\Big[-2\Big(\sigma_{p2}^2+\beta_{p2}^2\Big)-2c_2\Big(\xi_2^4+4\xi_2^2\beta_{p2}^2+2\beta_{p2}^4\Big)+m_2\beta_{p2}^2\Big],$$

$$a_{6,6}=-\mu_2\Big[2\Big(2\tau_{p2}^2+\xi_{p2}^2\Big)-2c_2\Big(\xi_2^4-4\xi_2^2\gamma_{p2}^2+2\gamma_{p2}^4\Big)-m_2\gamma_{p2}^2\Big],$$

$$a_{6,7}=-\mu_2\Big[-2\Big(\sigma_{p2}^2+\beta_{p2}^2\Big)-2c_2\Big(\xi_2^4+4\xi_2^2\beta_{p2}^2+2\beta_{p2}^4\Big)+m_2\beta_{p2}^2\Big],$$

$$a_{6,8}=-\mu_2\Big[2\Big(2\tau_{p2}^2+\xi_{p2}^2\Big)-2c_2\Big(\xi_2^4-4\xi_2^2\gamma_{p2}^2+2\gamma_{p2}^4\Big)-m_2\gamma_{p2}^2\Big],$$

$$a_{6,9}=-\mu_2\Big[2\zeta_2\beta_{s2}+c_2\zeta_2\beta_{s2}\Big(\sigma_{s2}^2+2\zeta_2^2\Big)-m_2\zeta_2\beta_{s2}\Big],$$

$$a_{6,10}=-\mu_2\Big[2\zeta_2\gamma_{s2}i-c_2\zeta_2\gamma_{s2}\Big(\tau_{s2}^2-2\zeta_2^2\Big)i-m_2\zeta_2\gamma_{s2}i\Big],$$

$$a_{6,11}=-\mu_2\Big[-2\zeta_2\beta_{s2}-c_2\zeta_2\beta_{s2}\Big(\sigma_{s2}^2+2\zeta_2^2\Big)+m_2\zeta_2\beta_{s2}\Big],$$

$$a_{6,12}=-\mu_2\Big[-2\zeta_2\gamma_{s2}i+c_2\zeta_2\gamma_{s2}\Big(\tau_{s2}^2-2\zeta_2^2\Big)i+m_2\zeta_2\gamma_{s2}i\Big],$$

$$a_{7,1}=-2c_1\xi_1\beta_{p1}^2i\mu_1,\ a_{7,2}=2c_1\xi_1\gamma_{p1}^2i\mu_1,\ a_{7,3}=-c_1\beta_{s1}i\Big(\zeta_1^2-\beta_{s1}^2\Big)\mu_1,\ a_{7,4}=c_1\gamma_{s1}\Big(\zeta_1^2+\gamma_{s1}^2\Big)\mu_1,$$

$$a_{7,5}=2c_2i\xi_2\beta_{p2}^2\mu_2,\ a_{7,6}=-2c_2\xi_2\gamma_{p2}^2i\mu_2,\ a_{7,7}=2c_2\xi_2\beta_{p2}^2i\mu_2,\ a_{7,8}=-2c_2\xi_2\gamma_{p2}^2i\mu_2,$$

$$a_{7,9}=-c_2\beta_{s2}i\Big(\zeta_2^2-\beta_{s2}^2\Big)\mu_2,\ a_{7,10}=c_2\gamma_{s2}\Big(\zeta_2^2+\gamma_{s2}^2\Big)\mu_2,$$

$$a_{7,11}=c_2\beta_{s2}i\Big(\zeta_2^2-\beta_{s2}^2\Big)\mu_2,\ a_{7,12}=-c_2\gamma_{s2}\Big(\zeta_2^2+\gamma_{s2}^2\Big)\mu_2,$$

$$a_{8,1}=2c_1\beta_{p1}i\mu_1\Big(\sigma_{p1}^2+\beta_{p1}^2\Big),\ a_{8,2}=2\mu_1c_1\gamma_{p1}\Big(2\tau_{p1}^2+\xi_{p1}^2\Big),$$

$a_{8,3} = 2\mu_1 c_1 \beta_{s1}^2 i\zeta_1,\ a_{8,4} = -2c_1\mu_1\zeta_1\gamma_{s1}^2 i,\ a_{8,5} = 2\mu_2 c_2 \beta_{p2} i\left(\sigma_{p2}^2 + \beta_{p2}^2\right),$

$a_{8,6} = 2\mu_2 c_2 \gamma_{p2}\left(2\tau_{p2}^2 + \xi_{p2}^2\right),\ a_{8,7} = -2\mu_2 c_2 \beta_{p2} i\left(\sigma_{p2}^2 + \beta_{p2}^2\right),\ a_{8,8} = -2\mu_2 c_2 \gamma_{p2}\left(2\tau_{p2}^2 + \xi_{p2}^2\right),$

$a_{8,9} = -2\mu_2 c_2 \beta_{s2}^2 i\zeta_2,\ a_{8,10} = 2\mu_2 c_2 \gamma_{s2}^2 \zeta_2 i,\ a_{8,11} = 2\mu_2 c_2 \beta_{s2}^2 i\zeta_2,\ a_{8,12} = 2\mu_2 c_2 \gamma_{s2}^2 \zeta_2 i,$

$q_1 = \exp(i\beta_{p2}h),\ q_2 = \exp(-\gamma_{p2}h),\ q_3 = \exp(-i\beta_{p2}h),\ q_4 = \exp(\gamma_{p2}h),$

$q_5 = \exp(i\beta_{s2}h),\ q_6 = \exp(-\gamma_{s2}h),\ q_7 = \exp(-i\beta_{s2}h),\ q_8 = \exp(\gamma_{s2}h),$

$p_1 = \exp(i\beta_{p3}h),\ p_2 = \exp(-\gamma_{p3}h),\ p_3 = \exp(i\beta_{s3}h),\ p_4 = \exp(-\gamma_{s3}h),$

$a_{9,5} = a_{1,5}q_1,\ a_{9,6} = a_{1,6}q_2,\ a_{9,7} = a_{1,7}q_3,\ a_{9,8} = a_{1,8}q_4,\ a_{9,9} = a_{1,9}q_5,\ a_{9,10} = a_{1,10}q_6,\ a_{9,11} = a_{1,11}q_7,$

$a_{9,12} = a_{1,12}q_8,\ a_{9,13} = \xi_3 p_1,\ a_{9,14} = \xi_3 p_2,\ a_{9,15} = \beta_{s3}p_3,\ a_{9,16} = i\gamma_{s3}p_4,\ a_{10,5} = a_{2,5}q_1,$

$a_{10,6} = a_{2,6}q_2,\ a_{10,7} = a_{2,7}q_3,\ a_{10,8} = a_{2,8}q_4,\ a_{10,9} = a_{2,9}q_5,\ a_{10,10} = a_{2,10}q_6,\ a_{10,11} = a_{2,11}q_7,$

$a_{10,12} = a_{2,12}q_8,\ a_{10,13} = \beta_{p3}p_1,\ a_{10,14} = i\gamma_{p3}p_2,\ a_{10,15} = -\zeta_3 p_3,\ a_{10,16} = -\zeta_3 p_4,\ a_{11,5} = a_{3,5}q_1,$

$a_{11,6} = a_{3,6}q_2,\ a_{11,7} = a_{3,7}q_3,\ a_{11,8} = a_{3,8}q_4,\ a_{11,9} = a_{3,9}q_5,\ a_{11,10} = a_{3,10}q_6,\ a_{11,11} = a_{3,11}q_7,$

$a_{11,12} = a_{3,12}q_8,\ a_{11,13} = -\xi_3\beta_{p3}p_1,\ a_{11,14} = -i\xi_3\gamma_{p3}p_2,\ a_{11,15} = -\beta_{s3}^2 p_3,\ a_{11,16} = \gamma_{s3}^2 p_4,$

$a_{12,5} = a_{4,5}q_1,\ a_{12,6} = a_{4,6}q_2,\ a_{12,7} = a_{4,7}q_3,\ a_{12,8} = a_{4,8}q_4,\ a_{12,9} = a_{4,9}q_5,\ a_{12,10} = a_{4,10}q_6,$

$a_{12,11} = a_{4,11}q_7,\ a_{12,12} = a_{4,12}q_8,\ a_{12,13} = -\beta_{p3}^2 p_1,\ a_{12,14} = \gamma_{p3}^2 p_2,\ a_{12,15} = \zeta_3\beta_{s3}p_3,$

$a_{12,16} = i\zeta_3\gamma_{s3}p_4,\ a_{13,5} = a_{5,5}q_1,\ a_{13,6} = a_{5,6}q_2,\ a_{13,7} = a_{5,7}q_3,\ a_{13,8} = a_{5,8}q_4,\ a_{13,9} = a_{5,9}q_5,$

$a_{13,10} = a_{5,10}q_6,\ a_{13,11} = a_{5,11}q_7,\ a_{13,12} = a_{5,12}q_8,$

$a_{13,13} = \mu_3\left[-2\xi_3\beta_{p3} - 2c_3\xi_3\beta_{p3}\left(2\sigma_{p3}^2 + \xi_3^2\right) + m_3\xi_3\beta_{p3}\right]p_1,$

$a_{13,14} = \mu_3\left[-2\xi_3\gamma_{p3}i + 2c_3\xi_3\gamma_{p3}\left(2\tau_{p3}^2 - \xi_3^2\right)i + m_3\xi_3\gamma_{p3}i\right]p_2,$

$a_{13,15} = \mu_3\left[\left(\zeta_3^2 - \beta_{s3}^2\right) - c_3\left(\beta_{s3}^4 - \zeta_3^4 + 2\zeta_3^2\beta_{s3}^2\right) + m_3\beta_{s3}^2\right]p_3,$

$a_{13,16} = \mu_3\left[\left(\zeta_3^2 + \gamma_{s3}^2\right) - c_3\left(\gamma_{s3}^4 - \zeta_3^4 - 2\zeta_3^2\gamma_{s3}^2\right) - m_3\gamma_{s3}^2\right]p_4,$

$a_{14,5} = a_{6,5}q_1,\ a_{14,6} = a_{6,6}q_2,\ a_{14,7} = a_{6,7}q_3,\ a_{14,8} = a_{6,8}q_4,\ a_{14,9} = a_{6,9}q_5,\ a_{14,10} = a_{6,10}q_6,$

$a_{14,11} = a_{6,11}q_7,\ a_{14,12} = a_{14,12}q_8,$

$a_{14,13} = \mu_3\left[-2\left(\sigma_{p3}^2 + \beta_{p3}^2\right) - 2c_3\left(\xi_3^4 + 4\xi_3^2\beta_{p3}^2 + 2\beta_{p3}^4\right) + m_3\beta_{p3}^2\right]p_1,$

$a_{14,14} = \mu_3\left[2\left(2\tau_{p3}^2 + \xi_{p3}^2\right) - 2c_3\left(\xi_3^4 - 4\xi_3^2\gamma_{p3}^2 + 2\gamma_{p3}^4\right) - m_3\gamma_{p3}^2\right]p_2,$

$a_{14,15} = \mu_3\left[2\zeta_3\beta_{s3} + c_3\zeta_3\beta_{s3}\left(\sigma_{s3}^2 + 2\zeta_3^2\right) - m_3\zeta_3\beta_{s3}\right]p_3,$

$a_{14,16} = \mu_3\left[2\zeta_3\gamma_{s3}i - c_3\zeta_3\gamma_{s3}\left(\tau_{s3}^2 - 2\zeta_3^2\right)i - m_3\zeta_3\gamma_{s3}i\right]p_4,$

$a_{15,5} = a_{7,5}q_1,\ a_{15,6} = a_{7,6}q_2,\ a_{15,7} = a_{7,7}q_3,\ a_{15,8} = a_{7,8}q_4,\ a_{15,9} = a_{7,9}q_5,\ a_{15,10} = a_{7,10}q_6,$

$a_{15,13} = -2i\mu_3 c_3 \beta_{p3}^2 \xi_3 p_1,\ a_{15,14} = 2\mu_3 c_3 \gamma_{p3}^2 \xi_3 i p_2,$

$a_{15,15} = \mu_3 c_3 \beta_{s3} i\left(\zeta_3^2 - \beta_{s3}^2\right)p_3,\ a_{15,16} = -\mu_3 c_3 \gamma_{s3}\left(\zeta_3^2 + \gamma_{s3}^2\right)p_4,$

$a_{16,5} = a_{8,5}q_1,\ a_{16,6} = a_{8,6}q_2,\ a_{16,7} = a_{8,7}q_3,\ a_{16,8} = a_{7,8}q_4,\ a_{16,9} = a_{8,9}q_5,\ a_{16,10} = a_{8,10}q_6,$

$a_{15,11} = a_{7,11}q_7,\ a_{15,12} = a_{7,12}q_8,\ a_{16,11} = a_{8,11}q_7,\ a_{16,12} = a_{8,12}q_8,$

$a_{16,13} = -2\mu_3 c_3 \beta_{p3} i\left(\sigma_{p3}^2 + \beta_{p3}^2\right)p_1,\ a_{16,14} = -2\mu_3 c_3 \gamma_{p3}\left(2\tau_{p3}^2 + \xi_{p3}^2\right)p_2,$

$a_{16,15} = 2\mu_3 c_3 \beta_{s3}^2 \zeta_3 i p_3,\ a_{16,16} = -2c_3\mu_3\zeta_3\gamma_{s3}^2 i p_4,$

$a_{ij} = 0\ (i = 1, \cdots, 8, ;\ j = 13, \cdots, 16)\ and\ (i = 9, \cdots, 16;\ j = 1, \cdots, 4)$

$b_{11} = -\xi_1,\ b_{21} = -\beta_{p1},\ b_{31} = \xi_1\beta_{p1},\ b_{41} = \beta_{p1}^2,$

$$b_{51} = -\mu_1\Big[-2\xi_1\beta_{p1} - 2c_1\xi_1\beta_{p1}\left(2\sigma_{p1}^2 + \xi_1^2\right) + m_1\xi_1\beta_{p1}\Big],$$

$$b_{61} = -\mu_1\Big[-2\left(\sigma_{p1}^2 + \beta_{p1}^2\right) - 2c_1\left(\xi_1^4 + 4\xi_1^2\beta_{p1}^2 + 2\beta_{p1}^4\right) + m_1\beta_{p1}^2\Big],$$

$$b_{71} = 2c_1\xi_1\beta_{p1}^2 i\mu_1,\ b_{81} = 2\mu_1 c_1\beta_{s1} i\zeta_1\left(\sigma_{p1}^2 + \beta_{p1}^2\right),\ b_{l1} = 0\ (l = 9, \cdots, 16)$$

where

$$\xi_1 = \sigma_{p1}\sin\theta_1,\ \beta_{p1} = \sigma_{p1}\cos\theta_1,\ \zeta_1 = \sigma_{s1}\sin\theta_2,\ \beta_{s1} = \sigma_{s1}\cos\theta_2,$$

$$\xi_2 = \sigma_{p2}\sin\theta_p,\ \beta_{p2} = \sigma_{p2}\cos\theta_p,\ \zeta_2 = \sigma_{s2}\sin\theta_s,\ \beta_{s2} = \sigma_{s2}\cos\theta_s,$$

$$\xi_3 = \sigma_{p3}\sin\theta_3,\ \beta_{p3} = \sigma_{p3}\cos\theta_3,\ \zeta_3 = \sigma_{s3}\sin\theta_4,\ \beta_{s3} = \sigma_{s3}\cos\theta_4.$$

References

Arkadi, Berezovski, Mihhail, Berezovski, 2013. Influence of microstructure on thermoelastic wave propagation. Acta Mech. 224, 2623–2633.

Askes, Harm, Aifantis, Elias C., 2011. Gradient elasticity in statics and dynamics: an overview of formulations, length scale identification procedures, finite element implementations and new results. Int. J. Solids Struct. 48, 1962–1990.

Chong, A.C.M., Lam, D.C.C., 1999. Strain gradient plasticity effete in indentation hardness of polymers. J. Mater. Res. 14 (10), 4103–4110.

Eringen, A.C., 1964. Mechanics of micromorphic materials. In: Gortler, H. (Ed.), Proc. XI, Int. Congress of Applied Mechanics. Springer Verlag, New York.

Eringen, A.C., 1966. Linear theory of micropolar elasticity. J. Math. Mech. 15, 909–924.

Eringen, A.C., 1990. Theory of thermo-microstretch elastic solids. Int. J. Eng. Sci. 28, 1291–1301.

Eringen, A.C., 2001. Nonlocal Continuum Field Theories. Springer-Verlag, Berlin, Heidelberg.

Fleck, N.A., Muller, G.M., Ashby, M.F., et al., 1994. Strain gradient plasticity: theory and experiment. Acta Metall. Mater. 42 (2), 475–487.

Georgiadis, H.G., Vardoulakis, I., Velgaki, E.G., 2004. Dispersive Rayleigh-wave propagation in microstructured solids characterized by dipolar gradient elasticity. J. Elast. 74, 17–45.

Giacomo, Caviglia, Angelo, Morro, 2008. Total reflection and tunneling of transient waves at a layer. Wave Motion 45, 278–292.

Giacomo, Caviglia, Angelo, Morro, 2012. Wave propagation and reflection-transmission in a stratified viscoelastic solid. Int. J. Solids Struct. 49, 567–575.

Gourgiotis, P.A., Georgiadis, H.G., Neocleous, I., 2013. On the reflection of waves in half-spaces of microstructured materials governed by dipolar gradient elasticity. Wave Motion 50, 437–455.

Hsia, Shao-Yi, Su, Chih-Chun, 2008. Propagation of longitudinal waves in microporous slab sandwiched between elastic half-spaces. Jpn. J. Appl. Phys. 7 (47), 5581–5590.

Khurana, Aarti, Tomar, S.K., 2009. Longitudinal wave response of a chiral slab interposed between micropolar solid half-spaces. Int. J. Solids Struct. 46, 135–150.

Larin, N.V., Tolokonnikov, L.A., 2006. The transmission of a plane acoustic wave through a non-uniform thermoelastic layer. J. Appl. Math. Mech. 70, 590–598.

McFarland, A.W., Colton, J.S., 2005. Role of material microstructure in plate stiffness with relevance to microcantilever sensors. J. Micromech. Microeng. 15 (5), 1060–1067.

Mindlin, R.D., 1964. Micro-structure in linear elasticity. Arch. Ration. Mech. Anal. 16, 51–78.

Mindlin, R.D., Tiersten, H.F., 1962. Effects of couple stress in linear elasticity. Arch. Ration. Mech. Anal. 11, 415–448.

Parfitt, V.R., Eringen, A.C., 1969. Reflection of plane waves from the flat boundary of a micropolar half-space. J. Acoust. Soc. Am. 45, 1258–1272.

Stölken, J.S., Evans, A.G., 1998. A microbend test method for measuring the plasticity length scale. Acta Mater. 46 (14), 5109–5115.

Tolokonnikov, L.A., 1998. The transmission of sound through an inhomogeneous anisotropic layer adjoining viscous liquids. J. Appl. Math. Mech. 6 (62), 953–958.

Tomar, S.K., Gogna, M.L., 1995. Reflection and refraction of longitudinal wave at an interface between two micropolar elastic solids at welded contact. J. Acoust. Soc. Am. 97 (2), 822–830.

Toupin, R.A., 1962. Elastic materials with couple stresses. Arch. Ration. Mech. Anal. 11, 385–414.